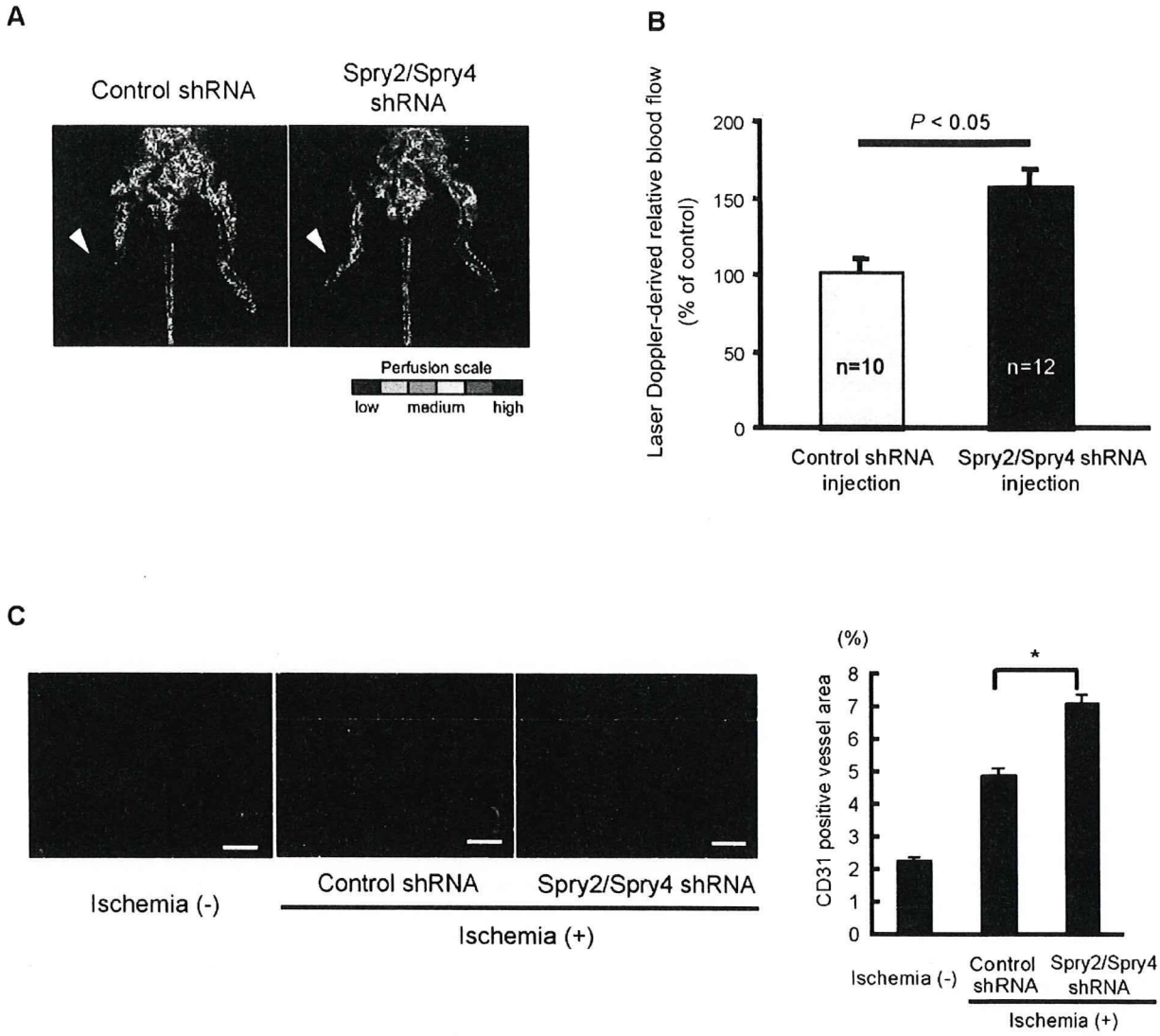

Figure 7. Increased ischemia-induced angiogenesis by *in vivo* shRNA targeting *Sprouty2 and Sprouty4*. (A) Representative laser Doppler images for each group are depicted. Arrowheads indicate ischemic limbs. The interval of low perfusion is displayed as dark blue; the highest perfusion interval is displayed as red. (B) Recovery of limb perfusion in C57BL/6J mice (8 weeks old) injected with the control shRNA (n = 10) or *Sprouty2/Sprouty4* shRNA vectors (n = 12) after hind limb ischemia as assessed by laser Doppler blood flow analysis on day 14. Data shown are means ± SD. *: $P<0.05$. (C) Blood vessels (green) in the non-ischemic or ischemic adductor muscle injected with the control shRNA or *Sprouty2/Sprouty4* shRNA vectors stained with anti-PECAM-1/CD31Ab. Nuclei were stained with Hoechst 33342 dye (blue). The CD31-positive vessel area was quantified. Data shown are means ± SEM. *: $P<0.05$. Scale bars (C): 100 μm.
doi:10.1371/journal.pone.0005467.g007

Plat-E, packaging cell line, transfected with pMX-VEGFR-2 or shRNA plasmids, and then the infected cells were selected with 1 μg/ml puromycin (Invivogen, San Diego, CA, USA), as previously described [18,35].

Antibodies and reagents

Antibodies used in this experiment were as follows: anti-phospho-ERK1/2 (#9106), anti-phospho-Akt (#4058), and anti-Akt (#9272) (Cell Signaling Technology, Danvers, MA, USA); anti-Sprouty4 (H-100), anti-VEGFR-2 (A-3) and anti-ERK2 (C-14) (Santa Cruz Biotechnology, Santa Cruz, CA, USA); anti-Sprouty2 (ab50317) (Abcam, Cambridge, MA, USA); and anti-vWF (DAKO, Glostrup, Denmark); Mouse VEGF-A was purchased from R&D Systems (Minneapolis, MN, USA). Human VEGF-A was purchased from PeproTech (London, UK).

RT-PCR and real-time PCR analysis

The cells or tissues were lysed in RNAiso (TAKARA BIO, Shiga, Japan) for RNA preparation. Total RNA was isolated through fluorescence activated cell sorting (FACS), which sorted about 5.0×10^4 BECs and LECs at embryonic day 14.5, as previously reported [18]. Good separation of BECs and LECs was confirmed by BEC markers (*Nrp1*, *CD44*) and LEC markers (*LYVE-1*, *Prox1*). Total RNA was reverse transcribed using the High Capacity cDNA Reverse Transcription Kit (Applied Biosystems, Foster City, CA, USA), and the product was used

for further analysis. PCR products were separated on 2.0% agarose gel stained with ethidium bromide. The expression level of *GAPDH* was evaluated as an internal control. The primer sequences for RT-PCR were as follows: *Sprouty2*-F, 5′- TTTTAATCCACCGATTGCTTGG-3′; *Sprouty2*-R, 5′-GCTGCACTCGGATTATTCCATC-3′; *Sprouty4*-F, 5′-CAGCTCCTCAAAGACCCCTAGAAGC-3′; *Sprouty4*-R, 5′-GTGCTGCTACTGCTGCTTACAGAGC-3′; *GAPDH*-F, 5′-ACCACAGTCCATGCCATCAC-3′ and *GAPDH*-R 5′-TCCACCACCCTGTTGCTGTA-3′. The primer sequences for BEC and LEC markers were described elsewhere [36]. Real-time PCR was performed on cDNA samples using an ABI 7000 Sequence Detection System (Applied Biosystems) with the SYBR Green system (Applied Biosystems). The relative quantitation value is expressed as 2^{-Ct}, where *Ct* is the difference between the mean *Ct* value of triplicates of the sample and of the endogenous *GAPDH* control. The primer sequences for real-time PCR were as follows: *Sprouty2*-F, 5′-ATAATCCGAGTGCAGCCTAAATC-3′; *Sprouty2*-R, 5′-CGCAGTCCTCACACCTGTAG-3′; *Sprouty4*-F, 5′-CGACCAGAGGCTCCTAGATCA-3′; *Sprouty4*-R, 5′-CAGCGGCTTACAGTGAACCA-3′; *GAPDH*-F, 5′-TGTGTCCGTCGTGGATCTGA-3′ and *GAPDH*-R 5′-CCTGCTTCACCACCTTCTTGA-3′.

Western blot analysis

Western blot analysis was performed as described previously [18]. MEFs were lysed in lysis buffer (50 mM Tris-HCl, pH 7.6, 150 mM NaCl, 1% Nonidet P-40, 1 mM sodium vanadate) supplemented with protease inhibitors (Nacalai tesque, Kyoto, Japan). About 20 μg of proteins were separated by SDS-PAGE and transferred to Immobilon-P nylon membranes (Millipore, Bedford, MA, USA).

Immunohistochemistry

Whole-mount immunohistochemistry of adult ears or immunohistochemistry of adult skin was performed with 1:200 diluted anti-PECAM-1/CD31 (MEC13.3, BD Pharmingen, Franklin Lakes, NJ, USA) or anti-LYVE-1 antibody (Acris Antibodies, Hiddenhausen, Germany) essentially as described previously [18].

Retinal angiography

Flat-mounted retinas were evaluated using fluorescein–dextran angiography as described elsewhere [22]. The mice were deeply anesthetized and a 0.03 ml/g body weight 50 mg/mL solution of 2×10^6 molecular weight FITC–dextran (Sigma, St Louis, MO, USA) was perfused through the left ventricle. The eyes were enucleated and fixed in 4% paraformaldehyde for at least 3 h. The corneas and lenses were then removed, and the peripheral retinas were dissected and flat-mounted on microscope slides for examination under a fluorescence microscope.

Vessel quantitative analysis

The vascular area in the ear, skin or muscle was quantified as a PECAM-1/CD31-positive area from ten ×10 micrographs, using Image J software (http://rsb.info.nih.gov), as described elsewhere [37]. LYVE-1-positive vessels in the skin were quantified in a similar manner.

RNAi-mediated knockdown

The mammalian expression vector pSUPER.retro.puro (Oligoengine, Seattle, WA, USA) was used for expression of shRNA targeting murine *Sprouty2*. The sequence of the *Sprouty2* shRNA is 5′-GCCGGGTTGTCGTTGTAAA-3′ and corresponds to nucleotides 1150–1168 of *mSprouty2*. Murine *Sprouty4* shRNA (29-mer) and control plasmids were purchased from Origene (Rockville, MD, USA) and used according to the manufacturer's protocols. The specificity of *Sprouty2* and *Sprouty4* knockdown was confirmed by real-time PCR or immunoblotting of whole-cell lysates of MEFs with anti-Sprouty2 and anti-Sprouty4 antibodies, respectively. The relative intensities of Sprouty2 or Sprouty4 band were normalized by STAT5 expression using Image J software, as previously described [9,35].

In vivo models of ischemia

A hind limb ischemia model was performed as previously described [23,38]. Male WT and *Sprouty4* KO mice (8–10 weeks old) and male C57BL/6J mice (8 weeks old) were used for a hind limb ischemia model. The proximal portion of the right femoral artery including the superficial and the deep branch and the distal portion of the saphenous artery were occluded with an electrical coagulator. After 2 weeks, we determined the ischemic (right)/nonischemic (left) limb blood flow ratio by using a laser Doppler blood flow imager (Laser Doppler Perfusion Imager System, moorLDI-Mark 2; Moor Instruments, Wilmington, DE, USA). Before initiating scanning, mice were placed on a heating pad at 37°C to minimize variations in their body temperatures. Calculated perfusion is expressed as the ratio of ischemic to nonischemic hind limb perfusion. At 2 wk after femoral resection, adductor muscles from the ischemic and control limbs were embedded in OCT compound. Eight-micron sections were stained with anti-PECAM-1/CD31 antibody (BD Pharmingen) and anti-rat Ig secondary antibody. For *in vivo* shRNA targeting *Sprouty2* and *Sprouty4*, a hind limb ischemia model was performed. Immediately after ischemia was induced, either a total of 40 μg *Sproutys* shRNA vectors (20 μg *Sprouty2* shRNA vector and 20 μg *Sprouty4* shRNA vector) or a quantity of control shRNA vectors was injected into five different sites in the adductor muscle of each anesthetized mouse [32]. A model of soft tissue ischemia similar to one described elsewhere [24,39] was developed. The model consisted of lateral skin incisions (2.5 cm in length and 1.25 cm apart) created on the dorsal surface of mice, penetrating the skin, dermis, and underlying adipose tissue. The overlying skin was undermined, and a 0.13-mm-thick silicone sheet was inserted to separate the skin from the underlying tissue bed. The skin was then reapproximated with 6-0 nylon sutures.

Corneal micropocket assay

The mouse corneal micropocket assay and quantification of neovascularization were performed as described elsewhere [40], using male BALB/c mice (6–10 weeks old). For local delivery, shRNA plasmids (total 10 μg/10 μl per eye) were diluted in phosphate-buffered saline (PBS) and delivered subconjunctivally. The subconjunctival injections were given after hydron pellet implantation.

Statistical analysis

Data are expressed as mean±SD or mean±SEM. Statistical significance was tested with an unpaired two-tailed Student's *t*-test or analysis of variance (ANOVA). The differences were considered to be significant if $P<0.05$.

Acknowledgments

We thank T. Yoshioka, K. Fukuse, M. Asakawa, N. Shiino, H. Fujii, N. Kinoshita, M. Ohtsu, and Y. Yamada for technical assistance, and Y. Nishi and N. Soma for manuscript preparation. We also thank Dr. H. Nishinakamura for technical advice.

Author Contributions

Conceived and designed the experiments: KT HY TI HK YS MO YY AY. Performed the experiments: KT KiS KW TA FO RiK. Analyzed the data: KT KiS KW RiK. Contributed reagents/materials/analysis tools: KT TI RK. Wrote the paper: KT AY.

References

1. Kim HJ, Bar-Sagi D (2004) Modulation of signalling by Sprouty: a developing story. Nat Rev Mol Cell Biol 5: 441–450.
2. Mason JM, Morrison DJ, Basson MA, Licht JD (2006) Sprouty proteins: multifaceted negative-feedback regulators of receptor tyrosine kinase signaling. Trends Cell Biol 16: 45–54.
3. Cabrita MA, Christofori G (2008) Sprouty proteins, masterminds of receptor tyrosine kinase signaling. Angiogenesis 11: 53–62.
4. Takahashi T, Yamaguchi S, Chida K, Shibuya M (2001) A single autophosphorylation site on KDR/Flk-1 is essential for VEGF-A-dependent activation of PLC-gamma and DNA synthesis in vascular endothelial cells. Embo J 20: 2768–2778.
5. Hacohen N, Kramer S, Sutherland D, Hiromi Y, Krasnow MA (1998) sprouty encodes a novel antagonist of FGF signaling that patterns apical branching of the Drosophila airways. Cell 92: 253–263.
6. Casci T, Vinos J, Freeman M (1999) Sprouty, an intracellular inhibitor of Ras signaling. Cell 96: 655–665.
7. Wakioka T, Sasaki A, Kato R, Shouda T, Matsumoto A, et al. (2001) Spred is a Sprouty-related suppressor of Ras signalling. Nature 412: 647–651.
8. Kato R, Nonami A, Taketomi T, Wakioka T, Kuroiwa A, et al. (2003) Molecular cloning of mammalian Spred-3 which suppresses tyrosine kinase-mediated Erk activation. Biochem Biophys Res Commun 302: 767–772.
9. Brems H, Chmara M, Sahbatou M, Denayer E, Taniguchi K, et al. (2007) Germline loss-of-function mutations in SPRED1 cause a neurofibromatosis 1-like phenotype. Nat Genet 39: 1120–1126.
10. Flamme I, Frolich T, Risau W (1997) Molecular mechanisms of vasculogenesis and embryonic angiogenesis. J Cell Physiol 173: 206–210.
11. Folkman J (1995) Angiogenesis in cancer, vascular, rheumatoid and other disease. Nat Med 1: 27–31.
12. Hanahan D (1997) Signaling vascular morphogenesis and maintenance. Science 277: 48–50.
13. Shibuya M (2008) Vascular endothelial growth factor-dependent and -independent regulation of angiogenesis. BMB Rep 41: 278–286.
14. Hannun YA, Obeid LM (2008) Principles of bioactive lipid signalling: lessons from sphingolipids. Nat Rev Mol Cell Biol 9: 139–150.
15. Impagnatiello MA, Weitzer S, Gannon G, Compagni A, Cotten M, et al. (2001) Mammalian sprouty-1 and -2 are membrane-anchored phosphoprotein inhibitors of growth factor signaling in endothelial cells. J Cell Biol 152: 1087–1098.
16. Lee SH, Schloss DJ, Jarvis L, Krasnow MA, Swain JL (2001) Inhibition of angiogenesis by a mouse sprouty protein. J Biol Chem 276: 4128–4133.
17. Sasaki A, Taketomi T, Kato R, Saeki K, Nonami A, et al. (2003) Mammalian Sprouty4 suppresses Ras-independent ERK activation by binding to Raf1. Nat Cell Biol 5: 427–432.
18. Taniguchi K, Kohno R, Ayada T, Kato R, Ichiyama K, et al. (2007) Spreds are essential for embryonic lymphangiogenesis by regulating vascular endothelial growth factor receptor 3 signaling. Mol Cell Biol 27: 4541–4550.
19. Ayada T, Taniguchi K, Okamoto F, Kato R, Komune S, et al. (2009) Sprouty4 negatively regulates protein kinase C activation by inhibiting phosphatidylinositol 4,5-biphosphate hydrolysis. Oncogene 28: 1076–1088.
20. Sasaki A, Taketomi T, Wakioka T, Kato R, Yoshimura A (2001) Identification of a dominant negative mutant of Sprouty that potentiates fibroblast growth factor- but not epidermal growth factor-induced ERK activation. J Biol Chem 276: 36804–36808.
21. Taniguchi K, Ayada T, Ichiyama K, Kohno R, Yonemitsu Y, et al. (2007) Sprouty2 and Sprouty4 are essential for embryonic morphogenesis and regulation of FGF signaling. Biochem Biophys Res Commun 352: 896–902.
22. D'Amato R, Wesolowski E, Smith LE (1993) Microscopic visualization of the retina by angiography with high-molecular-weight fluorescein-labeled dextrans in the mouse. Microvasc Res 46: 135–142.
23. Sasaki K, Heeschen C, Aicher A, Ziebart T, Honold J, et al. (2006) Ex vivo pretreatment of bone marrow mononuclear cells with endothelial NO synthase enhancer AVE9488 enhances their functional activity for cell therapy. Proc Natl Acad Sci U S A 103: 14537–14541.
24. Tepper OM, Capla JM, Galiano RD, Ceradini DJ, Callaghan MJ, et al. (2005) Adult vasculogenesis occurs through in situ recruitment, proliferation, and tubulization of circulating bone marrow-derived cells. Blood 105: 1068–1077.
25. Taketomi T, Yoshiga D, Taniguchi K, Kobayashi T, Nonami A, et al. (2005) Loss of mammalian Sprouty2 leads to enteric neuronal hyperplasia and esophageal achalasia. Nat Neurosci 8: 855–857.
26. Sivak JM, Petersen LF, Amaya E (2005) FGF signal interpretation is directed by Sprouty and Spred proteins during mesoderm formation. Dev Cell 8: 689–701.
27. Wang S, Aurora AB, Johnson BA, Qi X, McAnally J, et al. (2008) The endothelial-specific microRNA miR-126 governs vascular integrity and angiogenesis. Dev Cell 15: 261–271.
28. Fish JE, Santoro MM, Morton SU, Yu S, Yeh RF, et al. (2008) miR-126 regulates angiogenic signaling and vascular integrity. Dev Cell 15: 272–284.
29. Kuhnert F, Mancuso MR, Hampton J, Stankunas K, Asano T, et al. (2008) Attribution of vascular phenotypes of the murine Egfl7 locus to the microRNA miR-126. Development 135: 3989–3993.
30. Schalch P, Patejunas G, Retuerto M, Sarateanu S, Milbrandt J, et al. (2004) Homozygous deletion of early growth response 1 gene and critical limb ischemia after vascular ligation in mice: evidence for a central role in vascular homeostasis. J Thorac Cardiovasc Surg 128: 595–601.
31. Masaki I, Yonemitsu Y, Yamashita A, Sata S, Tanii M, et al. (2002) Angiogenic gene therapy for experimental critical limb ischemia: acceleration of limb loss by overexpression of vascular endothelial growth factor 165 but not of fibroblast growth factor-2. Circ Res 90: 966–973.
32. Sugano M, Tsuchida K, Maeda T, Makino N (2007) SiRNA targeting SHP-1 accelerates angiogenesis in a rat model of hindlimb ischemia. Atherosclerosis 191: 33–39.
33. Antoine M, Wirz W, Tag CG, Mavituna M, Emans N, et al. (2005) Expression pattern of fibroblast growth factors (FGFs), their receptors and antagonists in primary endothelial cells and vascular smooth muscle cells. Growth Factors 23: 87–95.
34. Takeshita S, Isshiki T, Sato T (1996) Increased expression of direct gene transfer into skeletal muscles observed after acute ischemic injury in rats. Lab Invest 74: 1061–1065.
35. Nishinakamura H, Minoda Y, Saeki K, Koga K, Takaesu G, et al. (2007) An RNA-binding protein alphaCP-1 is involved in the STAT3-mediated suppression of NF-kappaB transcriptional activity. Int Immunol 19: 609–619.
36. Morisada T, Oike Y, Yamada Y, Urano T, Akao M, et al. (2005) Angiopoietin-1 promotes LYVE-1-positive lymphatic vessel formation. Blood 105: 4649–4656.
37. Tammela T, Zarkada G, Wallgard E, Murtomaki A, Suchting S, et al. (2008) Blocking VEGFR-3 suppresses angiogenic sprouting and vascular network formation. Nature 454: 656–660.
38. Chavakis E, Aicher A, Heeschen C, Sasaki K, Kaiser R, et al. (2005) Role of beta2-integrins for homing and neovascularization capacity of endothelial progenitor cells. J Exp Med 201: 63–72.
39. Kimura H, Miyashita H, Suzuki Y, Kobayashi M, Watanabe K, et al. (2009) Distinctive localization and opposed roles of vasohibin-1 and vasohibin-2 in the regulation of angiogenesis. Blood, in press.
40. Nakao S, Kuwano T, Tsutsumi-Miyahara C, Ueda S, Kimura YN, et al. (2005) Infiltration of COX-2-expressing macrophages is a prerequisite for IL-1 beta-induced neovascularization and tumor growth. J Clin Invest 115: 2979–2991.

The American Journal of Pathology, Vol. 175, No. 1, July 2009

DOI: 10.2353/ajpath.2009.080788

Vascular Biology, Atherosclerosis and Endothelium Biology

Vasohibin-1 Expression in Endothelium of Tumor Blood Vessels Regulates Angiogenesis

Tomoko Hosaka,*† Hiroshi Kimura,* Takahiro Heishi,* Yasuhiro Suzuki,* Hiroki Miyashita,* Hideki Ohta,‡ Hikaru Sonoda,‡ Takuya Moriya,§ Satoshi Suzuki,† Takashi Kondo,† and Yasufumi Sato*

From the Departments of Vascular Biology, and Thoracic Surgery,† Institute of Development, Aging and Cancer, Tohoku University, Sendai; the Discovery Research Laboratories,‡ Shionogi & Co., Ltd., Osaka; and the Department of Pathology,§ Tohoku University Hospital, Sendai, Japan*

In this study, we characterized the significance of the vascular endothelial growth factor-inducible angiogenesis inhibitor vasohibin-1 to tumors. In pathological sections of non-small cell lung carcinoma, vasohibin-1 was present in the endothelial cells of blood vessels of the tumor stroma, but not in the lymphatics. In cancer cells, the presence of vasohibin-1 was associated with hypoxia-inducible factor 1α/vascular endothelial growth factor and fibroblast growth factor-2 expression. We then examined the function of vasohibin-1 in the mouse by subcutaneously inoculating with Lewis lung carcinoma cells. Resultant tumors in *vasohibin-1*$^{-/-}$ mice contained more immature blood vessels and fewer apoptotic tumor cells than tumors in wild-type mice. In wild-type mice that had been inoculated with Lewis lung carcinoma cells, tail vein injection of adenovirus containing the human *vasohibin-1* gene inhibited tumor growth and tumor angiogenesis. Moreover, the remaining tumor vessels in adenoviral human *vasohibin-1* gene-treated mice were small, round, and mature, surrounded by mural cells. The addition of adenoviral human *vasohibin-1* gene to cisplatin treatment improved cisplatin's antitumor activity in mice. These results suggest that endogenous vasohibin-1 is not only involved in tumor angiogenesis, but when sufficient exogenous vasohibin-1 is supplied, it blocks sprouting angiogenesis by tumors, matures the remaining vessels, and enhances the antitumor effect of conventional chemotherapy. *(Am J Pathol 2009, 175:430–439; DOI: 10.2353/ajpath.2009.080788)*

Angiogenesis, also called neovascularization, is a fundamental process of blood vessel growth, and a hallmark of cancer development. Multiple studies show that tumor angiogenesis in non-small cell lung carcinoma (NSCLC) is associated with metastases and poor survival.[1] The importance of tumor angiogenesis is further emphasized by clinical studies of anti-angiogenic agents.[2] Indeed, anti-angiogenic therapy shows promise as an effective treatment for various cancers, including NSCLC.[3]

The local balance between angiogenesis stimulators and inhibitors regulates angiogenesis. The most important molecule that stimulates angiogenesis is vascular endothelial growth factor (VEGF).[4] The circulating level of VEGF before treatment predicts the survival of patients with NSCLC.[5–7] Hypoxia, one of the triggers of angiogenesis, induces the expression of various molecules including VEGF. Hypoxia frequently occurs in tumors due to the increased oxygen requirement of the proliferating cancer cells and the poor blood supply.[8] The induction of VEGF in the hypoxic condition is mediated by a transcription factor, hypoxia-inducible factor 1 (HIF1), a heterodimeric complex of HIF1α and HIF1β subunits. HIF1α is easily degraded under normoxic conditions, but becomes stable under hypoxic conditions, and makes a heterodimeric complex with HIF1β. The dimer binds to the hypoxia responsive element in the promoter of the VEGF gene.[9] A worse prognosis in patients with NSCLC is associated with increased expression of HIF1 in cancer cells.[10] Fibroblast growth factor (FGF)-2 is another growth factor that has potent angiogenic activity. The induction of FGF-2 in cancer cells is also associated with the angio-

Supported by a Grant-in-Aid for Scientific Research on Priority Areas from the Japanese Ministry of Education, Science, Sports and Culture, and by Health and Labor Sciences research grants, Third Term Comprehensive Control Research for Cancer, from the Ministry of Health, Labor, and Welfare (Japan).

Accepted for publication March 26, 2009.

Present Address of Takuya Moriya: Department of Pathology, Kawasaki Medical School Hospital, 577 Matsushima, Kurashiki 701-0192, Japan.

Address reprint requests to Yasufumi Sato, Department of Vascular Biology, Institute of Development, Aging and Cancer, Tohoku University, 4-1, Seiryo-machi, Aoba-ku, Sendai 980-8575, Japan. E-mail: y-sato@idac.tohoku.ac.jp.

Table 1. Patient Profile

Number of patients	44
Sex (%)	
Male	28 (63.6)
Female	16 (36.4)
Age	
Mean (range)	66.2 (45–82)
Histology (%)	
Adenocarcinoma	35 (79.5)
Squamous cell carcinoma	9 (20.5)
Stage (%)	
IA	29 (65.9)
IB	5 (11.3)
IIA	0 (0)
IIB	1 (2.3)
IIIA	7 (15.9)
IIIB	1 (2.3)
IV	1 (2.3)

Table 2. Relationship between VEGF and HIF-1α in NSCLCs

	VEGF Negative	VEGF Positive	Total
HIF-1α Negative	9	2	11
HIF-1α Positive	12	21	33
Total	21	23	44

genic switch.[11] Indeed, FGF-2 is expressed in some NSCLC cells.[5–7]

The activities of angiogenesis stimulators are normally countered by angiogenesis inhibitors. A number of angiogenesis inhibitors have been identified to date.[12] Thrombospondin 1 is the best-characterized angiogenesis inhibitor in NSCLC. The expression of thrombospondin 1 is under the control of p53.[13] In cancer cells including NSCLC, alteration of the p53 gene is associated with decreased expression of thrombospondin 1.[14] The decreased expression of thrombospondin 1 in NSCLC is confirmed by others,[15–17] and correlates with poor prognosis.[15]

We have recently isolated a novel angiogenesis inhibitor, vasohibin (VASH), from endothelial cells (ECs).[18] Because a homologue of VASH was reported as VASH2,[19] the prototype VASH is now called VASH1. The characteristic feature of VASH1 is that it is induced in ECs by VEGF and FGF-2, two potent angiogenic factors.[18,20] Here we characterize the significance of VASH1 in tumors. We first verify the localization of VASH1 in relation to HIF1α, VEGF, or FGF-2 in the pathological sections of NSCLC. We then evaluate the role of VASH1 in tumor angiogenesis in animal models. Our analysis reveals that endogenous VASH1 is expressed in ECs of tumor blood vessels, and it is involved in the termination of tumor angiogenesis. When applied exogenously, VASH1 inhibits sprouting angiogenesis in tumors, matures the remaining vessels, and enhances the antitumor effect of chemotherapy.

Materials and Methods

Materials

We used the following materials: anti-human CD31 monoclonal antibody (mAb), anti-human α-smooth muscle actin (αSMA) mAb, and Rabbit/Mouse Ig Immunohistochemistry Kit (DAKO Cytomation, Glostrup, Denmark); anti-human HIF-1α goat antibody (Ab), and anti-human

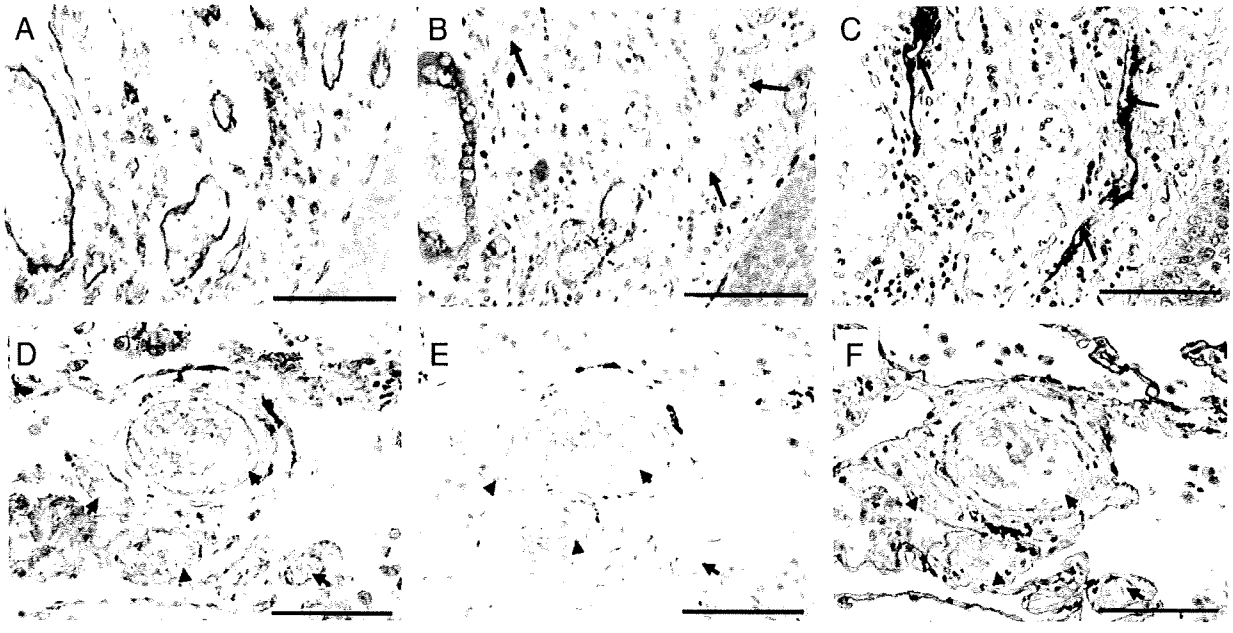

Figure 1. Presence of VASH1 in blood vessel ECs in the tumor stroma of NSCLCs. Pathological sections of NSCLC were immunostained for endothelial cell marker CD31 (**A** and **D**), VASH1 (**B** and **E**), and the lymphatic endothelial cell marker podoplanin (**C** and **F**). (**A**), (**B**) and (**C**) show tumor stroma, whereas (**D**), (**E**), and (**F**) show non-cancerous region in the same patient. Scale bar = 100 μm. VASH1 was present in blood vessel ECs in the tumor stroma of NSCLCs. **Arrows** indicate lymphatic vessels in tumor stroma and **arrowheads** indicate blood vessels in non-cancerous resion.

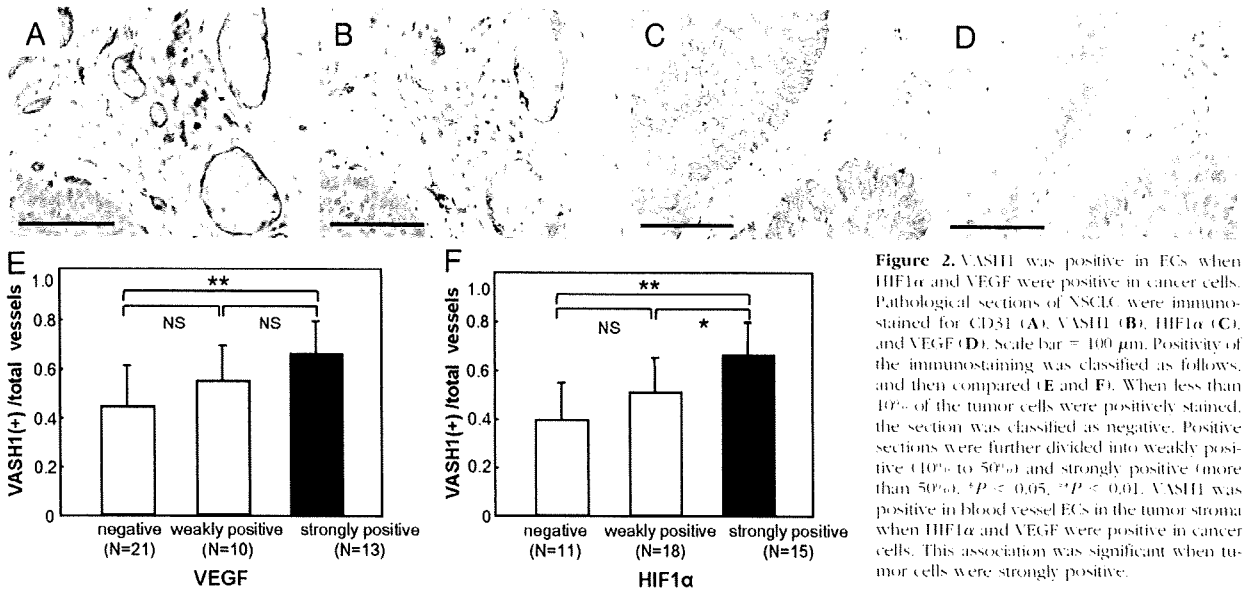

Figure 2. VASH1 was positive in ECs when HIF1α and VEGF were positive in cancer cells. Pathological sections of NSCLC were immunostained for CD31 (**A**), VASH1 (**B**), HIF1α (**C**), and VEGF (**D**). Scale bar = 100 μm. Positivity of the immunostaining was classified as follows, and then compared (**E** and **F**). When less than 10% of the tumor cells were positively stained, the section was classified as negative. Positive sections were further divided into weakly positive (10% to 50%) and strongly positive (more than 50%). $^{*}P < 0.05$, $^{**}P < 0.01$. VASH1 was positive in blood vessel ECs in the tumor stroma when HIF1α and VEGF were positive in cancer cells. This association was significant when tumor cells were strongly positive.

FGF-2 rabbit Ab (Santa Cruz Biotechnology, Santa Cruz, CA); anti-human podoplanin mAb (AngioBio, Del Mar, CA); anti-human VEGF mAb (LAB VISION, Fremont, CA); anti-human β-actin mAb, anti-mouse αSMA mAb, horseradish peroxidase-conjugated anti-mouse IgG and *cis*-diammineplatinum dichloride (CDDP) (Sigma, St. Louis, MO); anti-mouse CD31 rat Ab (Fitzgerald Industries International, Concord, MA); anti-mouse platelet-derived growth factor receptor β goat Ab (R&D Systems, Minneapolis, MN); biotin-conjugated anti-mouse or anti-goat IgG, IgA, IgM Ab, and streptavidin-biotin peroxidase complex (Nichirei Biosciences, Tokyo, Japan); Alexa fluor 568 labeled goat anti-rat IgG; Alexa 488 labeled donkey anti-mouse IgG; Alexa 488 labeled donkey anti-goat IgG; TO-PRO-3 iodide (Molecular Probes, Eugene, OR); OCT compound (Sakura Finetechnical, Tokyo, Japan); Dulbecco's modified Eagle's Medium (Nissui Pharmaceutical Co., Tokyo, Japan); fetal bovine serum (Equitech-Bio, Kerrville, TX); and diaminobenzidine (Sigma). Anti-human vasohibin-1 (VASH1) mAb was described previously.[18]

Patients

The clinical study included 44 patients with NSCLC, who underwent partial resection of a lung (lobectomy or pneumonectomy) in Tohoku University Hospital between November 2003 and January 2007. Informed consents were obtained from all of the patients, and the study was approved by the Ethical Committee of Tohoku University.

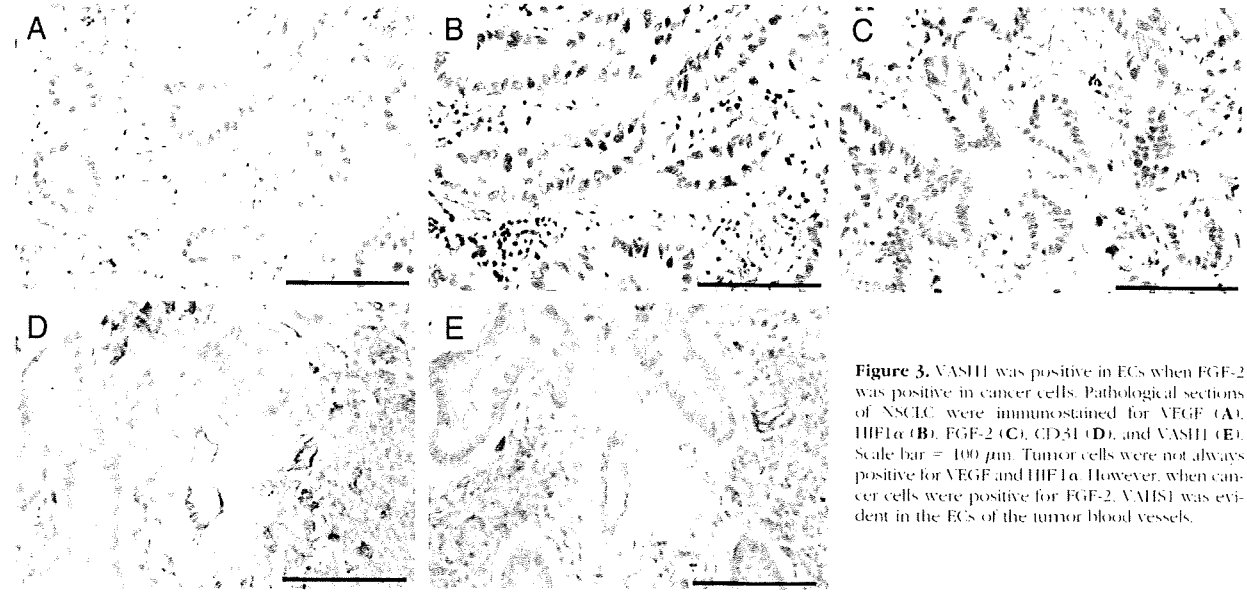

Figure 3. VASH1 was positive in ECs when FGF-2 was positive in cancer cells. Pathological sections of NSCLC were immunostained for VEGF (**A**), HIF1α (**B**), FGF-2 (**C**), CD31 (**D**), and VASH1 (**E**). Scale bar = 100 μm. Tumor cells were not always positive for VEGF and HIF1α. However, when cancer cells were positive for FGF-2, VASH1 was evident in the ECs of the tumor blood vessels.

Table 3. Relationship between VEGF and FGF-2 in NSCLCs

	VEGF Negative	VEGF Positive	Total
FGF-2 Negative	15	3	18
FGF-2 Positive	6	20	26
Total	21	23	44

Immunohistochemical Analysis of Human Lung Specimens

Human lung specimens were fixed in 10% formalin, embedded in paraffin, and cut into 3-μm thick sections. Sections were dewaxed in xylene, rehydrated in a graded ethanol series (100%, 90%, 80%, and 70%), and incubated in 10% H_2O_2/methanol to block endogenous peroxidase activity. Sections were then incubated in citrated buffer (pH 6.0) for 5 minutes at 121°C in a microwave oven for VASH1, CD31, and FGF-2 staining, in citrated buffer (pH 6.0); in the same conditions for 15 minutes for VEGF staining; and in 0.1% Trypsin/0.05 mol/L Tris buffer (pH 7.6) for 30 minutes at 37°C for αSMA staining. Thereafter, sections were incubated for 10 minutes at room temperature in a blocking solution of 10% rabbit or goat serum (Nichirei Biosciences). Primary antibody reactions were performed overnight at 4°C at a dilution of 1:400 for anti-human VASH1 mAb, 1:40 for anti-human CD31 mAb, 1:800 for anti-human αSMA mAb, 1:100 for anti-human HIF1α goat Ab, 1:200 for anti-human podoplanin mAb, 1:50 for anti-human VEGF mAb, and 1:200 for anti-FGF-2 rabbit Ab. A secondary antibody reaction was performed with biotin-conjugated anti-mouse or anti-goat IgG, IgA, and IgM Ab for 30 minutes at room temperature. Streptavidin-biotin peroxidase complex formation was performed for 30 minutes at room temperature. Sections were visualized using diaminobenzidine/H_2O_2 and sodium azide in 0.05mol/L Tris buffer, (pH 7.6). Nuclei were counterstained with hematoxylin.

To localize VASH1, mirror sections were prepared. One section was stained for CD31 and αSMA, and the other was stained for VASH1. For CD31 and αSMA, primary antibody reactions were performed overnight at 4°C; for anti-human CD31 mAb reactions were performed at day one. On day 2, sections were visualized using diaminobenzidine, 0.1 M/L glycine buffer (pH 2.2) for 30 minutes at room temperature. After treatment in 0.1% Trypsin, 0.05 mol/L Tris buffer, pH7.6, for 30 minutes at 37°C and washing with PBS three times, the sections underwent the primary antibody reaction for anti-human αSMA mAb overnight at 4°C. On day three, sections were visualized using 4 chloro-1naphtol and ethanol, 0.05 mol/L Tris buffer (pH 7.6)/H_2O_2, for 30 minutes at room temperature. After being washed with PBS three times, the sections were covered with aqueous mounting medium.

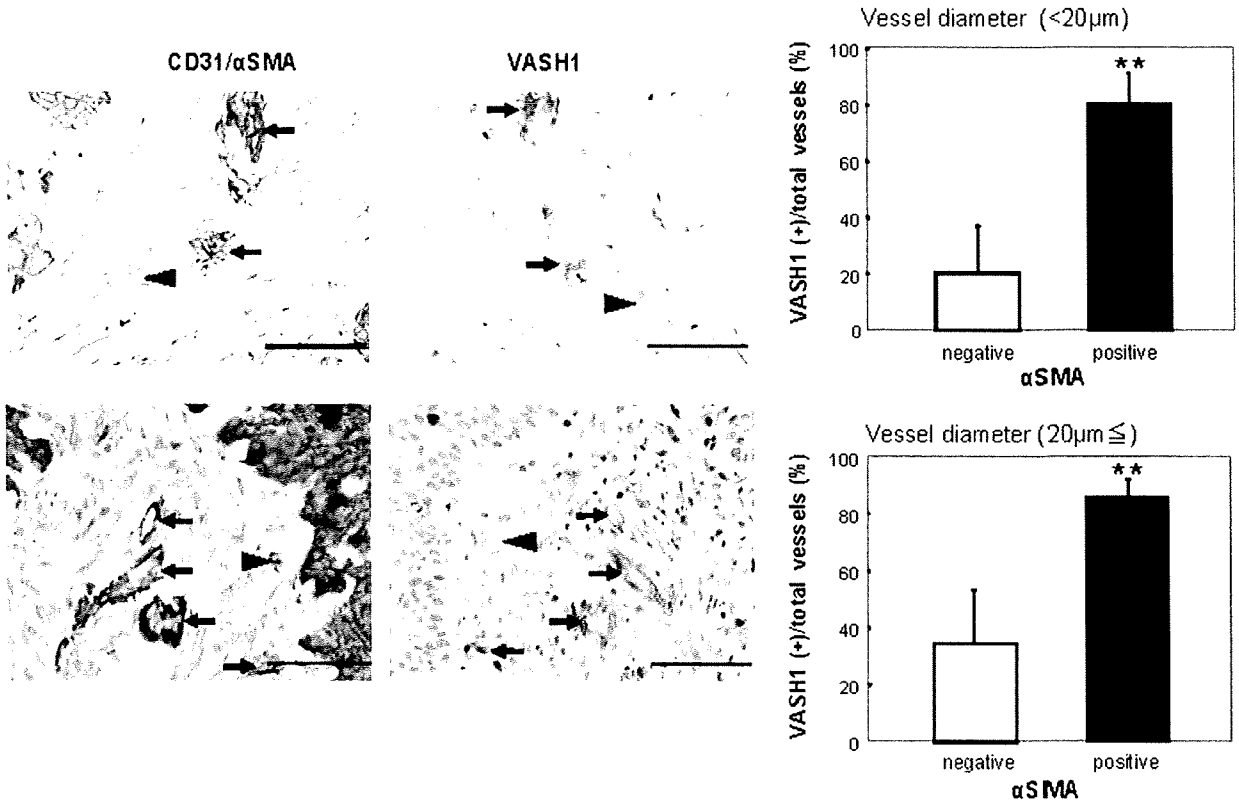

Figure 4. VASH1 was positive in ECs of tumor vessels when they were associated with mural cells. Mirror sections of NSCLC were immunostained for CD31 (brown) and αSMA (purple) on the left, and VASH1 (brown) on the right. Scale bar = 100 μm. VASH1 was positive when the vessels were associated with mural cell (**arrows**). VASH1 was negative when the vessel was not associated with mural cell (**arrowheads**). Quantification revealed that the positivity of VASH1 with mural cell association was evident regardless of the size of blood vessels. $^{**}P < 0.01$.

Interpretation of the Immunohistochemical Staining

Two pathologists evaluated all of the slides independently. To analyze CD31 and VASH1 staining, slides were scanned at low magnification (×100), and then vessels were counted in four random intratumoral areas of 1 mm^2, and in four random peritumoral areas of 1 mm^2. To determine HIF-1α, VEGF, and FGF-2 staining, slides were scanned at low magnification (×100). When less than 10% of the tumor cells were positively stained, the section was classified as negative; when more than 10% were positively stained, the section was classified as positive. In some cases, positive sections were further divided in to weakly positive (10% to 50%) and strongly positive (more than 50%).

Cells

Lewis lung carcinoma (LLC) cells were cultured in Dulbecco's modified Eagle's Medium supplemented with 10% fetal bovine serum, 100 μg/ml penicillin, 100 μg/ml streptomycin, and 4 mmol/L L-glutamine.[21]

Tumor Growth in Mice

Male C57 BJ/6 J mice, 6 to 8-week-old (Charles River, Japan) or *VASH1*$^{-/-}$ mice of C57 BJ/6 background[22]

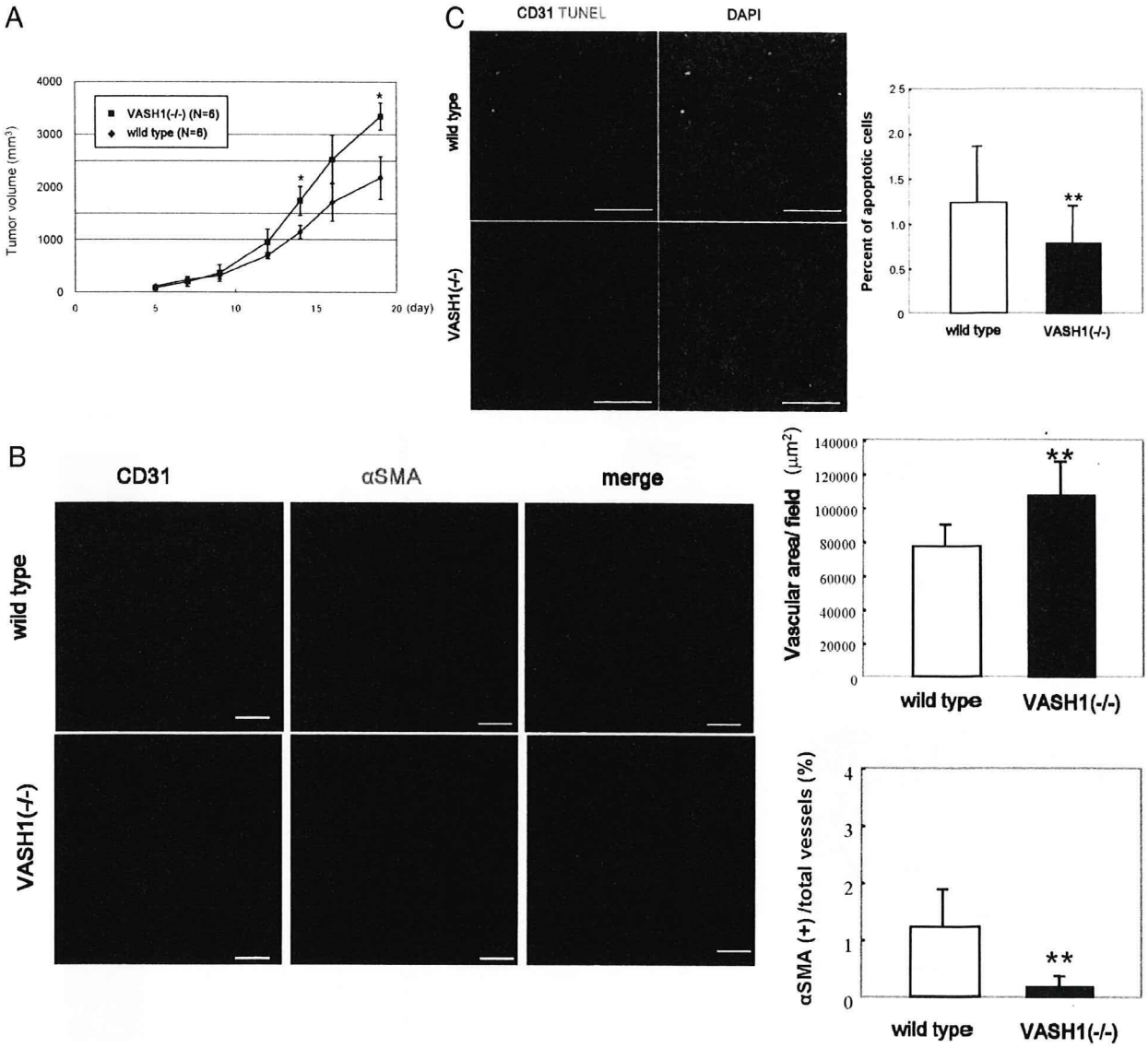

Figure 5. Tumor growth and tumor angiogenesis in *VASH1*$^{-/-}$ mice. **A:** LLC cells (5×10^6) were inoculated in wild-type and *VASH1*$^{-/-}$ mice, and tumor growth was evaluated. Data are expressed as the means and SDs. Tumors in *VASH1*$^{-/-}$ mice tended to grow bigger. $^*P < 0.05$. **B:** Tumor sections were co-immunostained for CD31 and αSMA. Tumors in *VASH1*$^{-/-}$ mice contained numerous small vessels. Scale bar = 100 μm. For this analysis, we counted 221 to 444 vessels per field (357 ± 66 per field) in wild-type and 328 to 780 vessels per field (472 ± 129 per field) in knockout mice. Quantification revealed that the vascularized tumor area in *VASH1*$^{-/-}$ mice was significantly increased, and vessels in *VASH1*$^{-/-}$ mice were more immature. $^{**}P < 0.01$. **C:** Apoptosis was evaluated by terminal deoxynucleotidyl transferase dUTP nick-end labeling. Scale bar = 100 μm. Tumors in *VASH1*$^{-/-}$ contained fewer apoptotic tumor cells. $^{**}P < 0.01$.

were inoculated in the subcutaneous tissue of the right abdominal wall with 5×10^6 LLC cells. Every 2 days after the inoculation, perpendicular tumor diameters were measured by digital calipers, and the tumor volume was calculated as 0.5 × length × width^2. At indicated periods after the inoculation, mice were sacrificed, and tumors were collected.

To evaluate the effect of VASH1, we used a replication-defective adenovirus vector encoding the human *VASH1* gene (AdVASH1). A replication-defective adenovirus vector encoding the *β-galactosidase* gene (AdLacZ) was used for the control.[18,23] A total of 100 μl AdVASH1 or AdLacZ, containing 1×10^9 plaque-forming units were injected into the mouse tail vein on day 7 after the inoculation. For the combination with CDDP, AdVASH1 or AdLacZ was injected in the tail vein at day 6 after the inoculation. The mice were then given an intraperitoneal injection of CDDP (2.5 mg/kg) on days 10, 14, and 18.[24,25]

Tumor tissues were embedded in OCT compound to make frozen tissue specimens, and sectioned at 7 μm. Sections were fixed with methanol for 20 minutes at 20°C, blocked with Protein Block Serum Free (DAKO Cytomation) for 10 minutes at room temperature, and stained with anti-mouse CD31 rat Ab (1:200), anti-mouse α-SMA mAb (1:200) or anti-mouse platelet-derived growth factor receptor (PDGFR) β goat Ab (1:10) overnight, followed by staining with Alexa fluor 568 labeled goat anti-Rat IgG (1:400), Alexa 488 labeled donkey anti-mouse IgG (1:400), Alexa 488 labeled donkey anti-goat IgG (1:400), and TO-PRO-3 iodide (1:1000) for 60 minutes at room temperature. After being washed with PBS three times, the sections were covered with fluorescent mounting medium. Terminal deoxynucleotidyl transferase dUTP nick-end labeling staining used Fluorescein FragEL DNA Fragmentation Detection Kit (EMD Chemicals Inc., Darmstadt, Germany) following manufacturer protocols. Stained samples were visualized using an Olympus FluoView FV1000 confocal microscope (Tokyo, Japan). The vascular lumen was traced and the luminal area was analyzed with NIH ImageJ software.

Statistical Analysis

Data are expressed as mean ± SD The statistical significance of differences was evaluated using the

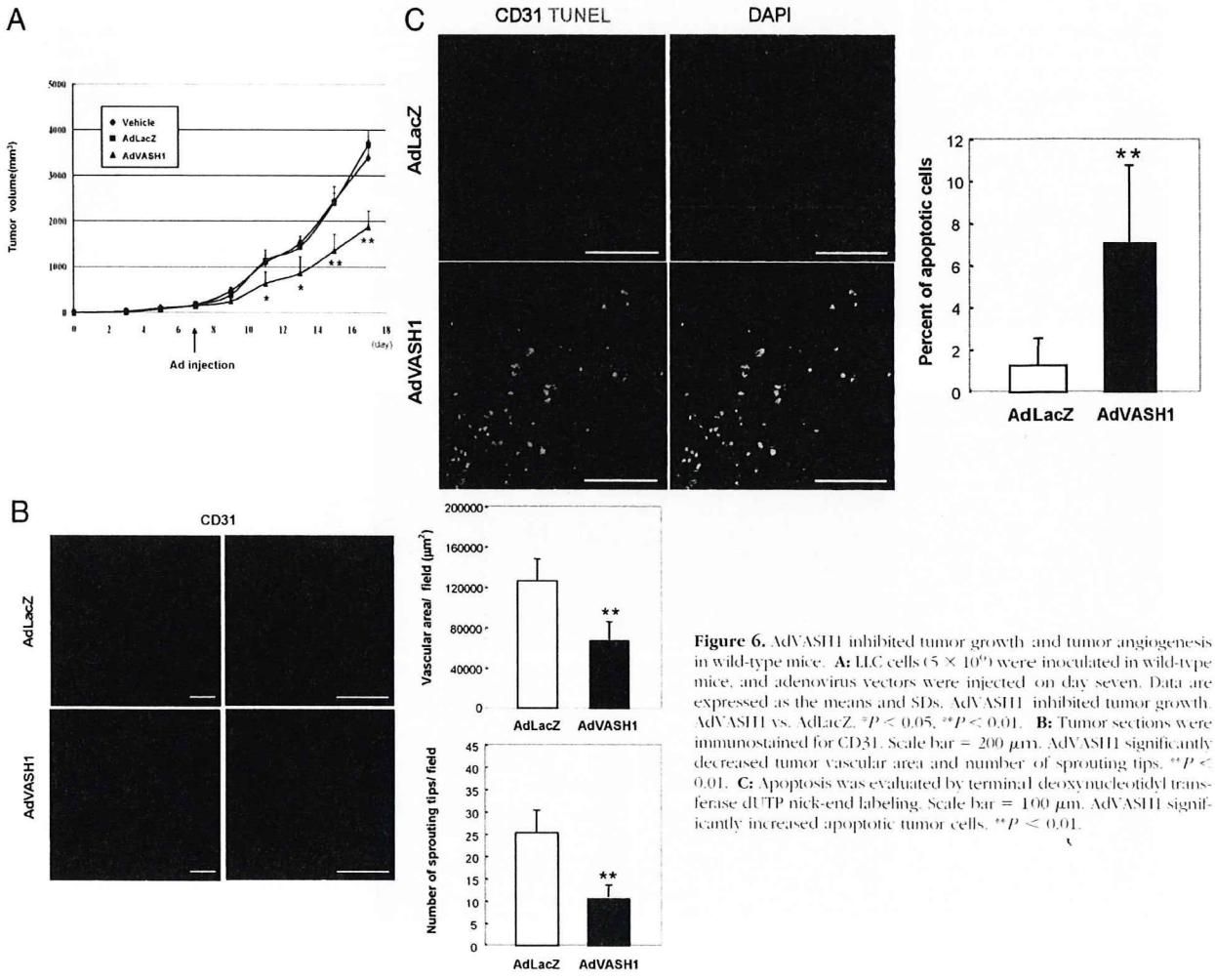

Figure 6. AdVASH1 inhibited tumor growth and tumor angiogenesis in wild-type mice. **A:** LLC cells (5×10^6) were inoculated in wild-type mice, and adenovirus vectors were injected on day seven. Data are expressed as the means and SDs. AdVASH1 inhibited tumor growth. AdVASH1 vs. AdLacZ. $^*P < 0.05$, $^{**}P < 0.01$. **B:** Tumor sections were immunostained for CD31. Scale bar = 200 μm. AdVASH1 significantly decreased tumor vascular area and number of sprouting tips. $^{**}P < 0.01$. **C:** Apoptosis was evaluated by terminal deoxynucleotidyl transferase dUTP nick-end labeling. Scale bar = 100 μm. AdVASH1 significantly increased apoptotic tumor cells. $^{**}P < 0.01$.

unpaired analysis of variance (analysis of variance), and P values were calculated using the unpaired Student's t-test. A value of $P < 0.05$ was accepted as statistically significant.

Results

Presence of VASH1 in Blood Vessel ECs in the Tumor Stroma of NSCLCs

We first evaluated the presence of VASH1 protein in human NSCLC specimens. The study included 44 patients with NSCLC (28 males and 16 females). Their average age was 66.2 years (range, 45 to 82 years). Based on the World Health Organization's criteria for tumor types, 35 patients had adenocarcinomas, and nine had squamous cell carcinomas. Twenty-nine patients had stage IA cancers, five patients had stage IB, one had stage II, eight had stage III, and one had stage IV cancers (Table 1).

Pathological sections of NSCLC were analyzed as follows. VASH1 was present in CD31 positive ECs, which were negative for lymphatic EC marker podoplanin (Figure 1A, C, D, and F). Thus, VASH1 is preferentially expressed in ECs of blood vessels. VASH1 was evident only in the tumor stroma (Figure 1B), and not in the non-cancerous region of the surgically resected tissue of the same patient (Figure 1E). This distinction indicates that the expression of this protein is closely associated with tumor blood vessels.

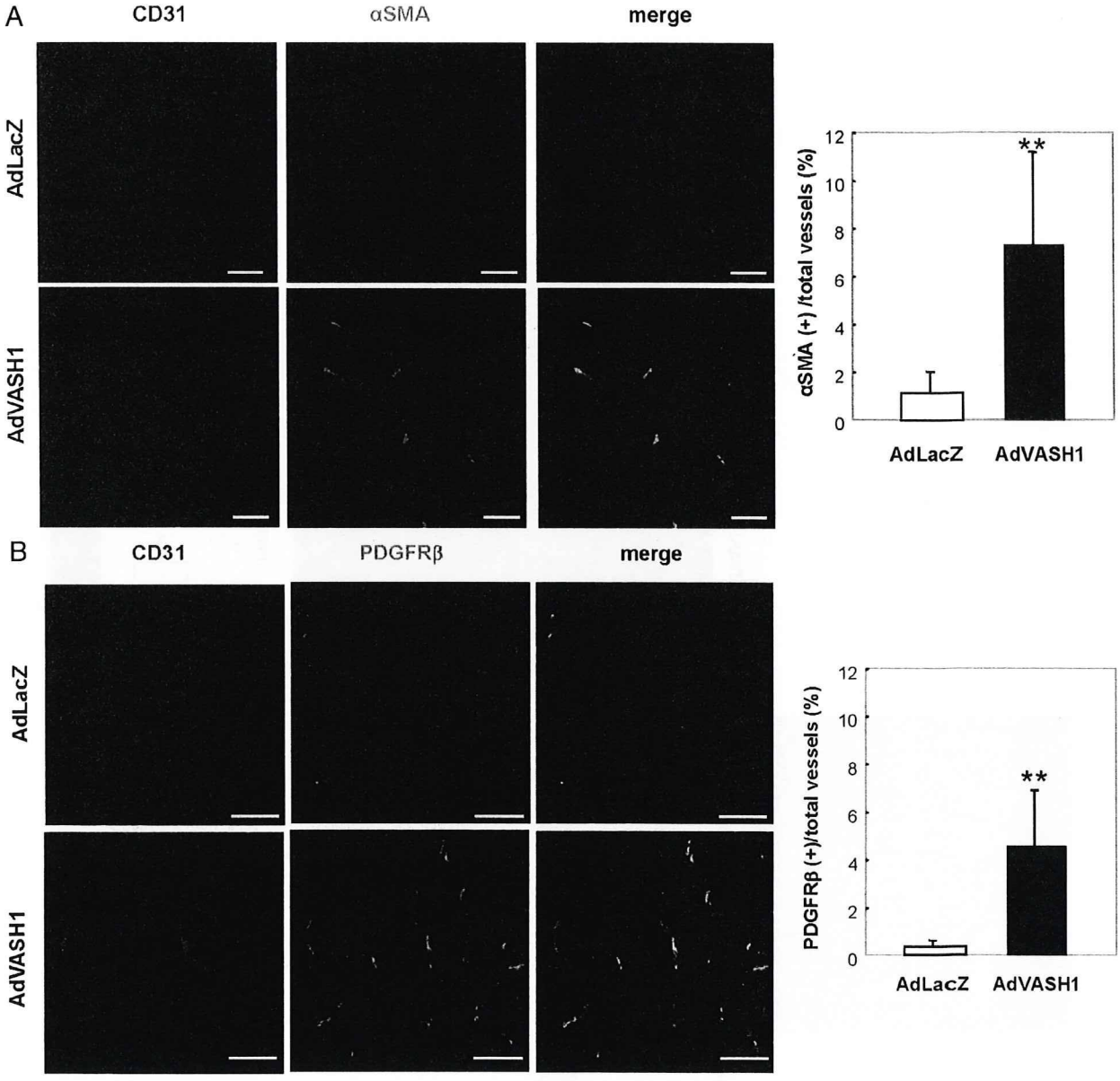

Figure 7. AdVASH1 matured tumor vessels in wild-type mice. Tumor sections were co-immunostained for (**A**) CD31 and αSMA or CD31 and (**B**) PDGFR β, an additional marker of mural cells. Scale bar = 100 μm. Tumor vessels in AdVASH1 injected mice were more frequently associated with mural cells. $^{**}P < 0.01$.

Relationship between VASH1 in ECs and VEGF or FGF-2 in Cancer Cells

Because VASH1 was inducible by two representative angiogenic factors, VEGF and FGF-2, in ECs,[18,20] we evaluated the relationships between VASH1 and VEGF or FGF-2. Because VEGF is induced in hypoxic conditions, the presence of VEGF was associated with the presence of HIF1α in cancer cells (Table 2).[26] Immunohistochemical analysis revealed that VASH1 was present in ECs in tumor blood vessels (Figure 2, A and B) when NSCLC cells were positive for VEGF and HIF-1α (Figure 2, C and D). Quantitative analysis confirmed that the presence of VASH1 in ECs was significantly higher in both VEGF positive and HIF1α positive tumors (Figure 2, E and F).

FGF-2 is another potent angiogenic factor. NSCLC cells were not always positive for VEGF. However, when cancer cells were positive for FGF-2, VASH1 was present in the ECs of tumor blood vessels (Figure 3A–E). The relationship between VEGF and FGF-2 is shown in Table 3.

Association of VASH1-Positive Tumor Vessels with Mural Cells

As we noticed that not all of the tumor blood vessels were positive for VASH1, we determined the characteristics of VASH1-positive tumor blood vessels. Immunostaining of αSMA in the mirror sections of NSCLC revealed that VASH1 was preferentially expressed in ECs when tumor blood vessels were associated with mural cells (Figure 4). Quantitative analysis further confirmed this association, independent of the sizes of the blood vessels (Figure 4).

Tumor Vessels in VASH1$^{-/-}$ Mice

The presence of endogenous VASH1 in tumor vessels promoted us to evaluate the function of this molecule in the animal model. When LLC cells were inoculated in *VASH1*$^{-/-}$ mice, tumors in *VASH1*$^{-/-}$ mice tended to grow bigger than in wild-type mice (Figure 5A). We then evaluated tumor vessels in *VASH1*$^{-/-}$ mice. The vascular area was increased and tumor vessels were more immature lacking mural cells in *VASH1*$^{-/-}$ mice (Figure 5B). Although the number of apoptotic cancer cells in wild-type mice was at a rather low level, it was further decreased in *VASH1*$^{-/-}$ mice (Figure 5C). These results indicate that endogenous VASH1 does function as an angiogenesis inhibitor in tumors.

Effect of Exogenous VASH1 on Tumor Growth and Tumor Angiogenesis

We next examined the effect of exogenous VASH1. We inoculated LLC cells into wild-type mice, and injected AdVASH1 in the tail vein 7 days later. This procedure supplies sufficient VASH1 protein to regulate angiogenesis as described previously.[23] AdLacZ was used as a negative control.[23] AdVASH1 injection significantly inhibited the growth of tumor in mice (Figure 6A). The immunohistochemical analysis revealed that the tumor vascular area was decreased and tumor cell apoptosis was augmented in the AdVASH1-treated mice (Figure 6, B and C). Moreover, the remaining tumor vessels in the AdVASH1-treated mice were small, round, and mature, associating with mural cells; whereas tumor vessels in the control AdLacZ-injected mice were dilated, erratic, and immature, containing sprouting endothelial cells with few mural cells (Figure 7, A and B).

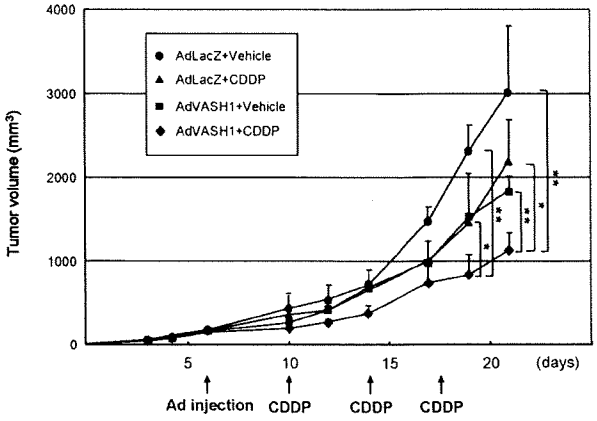

Figure 8. Anti-tumor activity of CDDP was enhanced when combined with AdVASH1. LLC cells (5×10^6) were inoculated in wild-type mice. Adenovirus vectors were injected on day seven, and CDDP (2.5 mg/kg) was injected on days 10, 14, and 18. Data are expressed as the means and SDs. AdVASH1 injection improved the anti-tumor effect of CDDP. $^*P < 0.05$, $^{**}P < 0.01$.

Because the VASH1 treatment caused the remaining tumor vessels to mature, we anticipated that those vessels would deliver anti-cancer drugs efficiently. We therefore tested the efficacy of the combination of VASH1 with CDDP. As expected, AdVASH1 injection improved the anti-tumor effect of CDDP (Figure 8).

Discussion

The search for molecular biomarkers of angiogenesis has been intensively pursued. Molecules that are specifically expressed in ECs can be candidates for such biomarkers. CD31, von Willebrand factor, and vascular endothelial-cadherin are used for histological identification of ECs.[27] However, those molecules are expressed in quiescent ECs as well, and thus cannot be specific for active angiogenesis. Endoglin and aminopeptidase N are expressed preferentially in ECs during angiogenesis.[28,29] Therefore, these two molecules are more suitable markers of angiogenesis. Additionally, several attempts have been made to isolate molecules that are expressed in cancer-specific ECs.[30–32] Nevertheless, such molecules had not been characterized in the clinical setting. In this report, we characterized the significance of VASH1, a VEGF-inducible angiogenesis inhibitor, in NSCLCs. Our data reveal that the expression of VASH1 was restricted to ECs of blood vessels in the tumor stroma, and was correlated with the expression of HIF-1α and VEGF, or FGF-2 in tumor cells. We have previously showed the presence of VASH1 in tumor vessels of human endome-

trial cancers as well.[33] We therefore propose that VASH1 should be further tested as a candidate of tumor angiogenesis biomarker.

We have previously determined the role of VASH1 in the mouse subcutaneous angiogenesis model.[22] Angiogenesis is normally synchronized and transient, as hypoxia-mediated angiogenic stimuli withdraw when blood starts to flow in the newly formed vessels. Our previous analysis in the mouse subcutaneous angiogenesis model has revealed that endogenous VASH1 is present in newly formed blood vessels behind the sprouting front where angiogenesis terminates (termination zone), and those VASH1-positive vessels are mature associated with mural cells.[22] As cancers contain complex lesions where angiogenesis is not synchronized and sprouting occurs randomly, it is difficult to dissect the spatio-temporal expression pattern of VASH1 in cancers. Here we show that VASH1 is prevalent in tumor blood vessels of NSCLC when they are associated with mural cells (Figure 4). This result suggests that the spatio-temporal expression profile of VASH1 is maintained even in tumor vessels.

Increased expression of angiogenesis stimulators, together with decreased expression of angiogenesis inhibitors, is proposed to occur in various cancers.[34] The presence of VASH1 in tumor vessels thus raises the question whether endogenous VASH1 acts as an angiogenesis inhibitor in tumors. We have previously demonstrated in the mouse subcutaneous angiogenesis model that the function of endogenous VASH1 is to terminate angiogenesis, but is not to inhibit angiogenesis in the sprouting front.[22] Here we compared tumors in wild-type and *VASH1*$^{-/-}$ mice. Tumors growth in wild-type mice was slower than in *VASH1*$^{-/-}$ mice. Histological analysis further demonstrated the distinction that tumors in *VASH1*$^{-/-}$ mice contained more immature vessels and fewer apoptotic tumor cells. This observation indicates that endogenous VASH1 does participate in the inhibition of tumor angiogenesis.

The persistence of sprouting ECs in tumor vessels in wild-type mice implies that endogenous VASH1 is ineffective in blocking sprouting angiogenesis in tumors. Importantly, when sufficient VASH1 is supplied exogenously, it can block angiogenesis in the sprouting front.[22] Here we show that sprouting ECs disappear from tumor vessels by the injection of AdVASH1. Tumor vessels in the control AdLacZ-injected mice were dilated, erratic and immature, containing fewer mural cells, whereas those in the AdVASH1-treated mice were small, round, and mature, associated with mural cells. These morphological differences imply that exogenous VASH1 has two modalities affecting tumor vessels. One is to inhibit sprouting angiogenesis, and the other is to participate in the termination of angiogenesis.

Abnormal tumor vessels bring about deficient blood flow within the tumor, which should impair the delivery of drugs to the tumor.[35] Maturation of tumor vasculature enhances the efficacy of cytotoxic anti-cancer therapies, as it increases the delivery of anti-cancer drugs to the tumor cells.[35] We therefore anticipated that exogenous VASH1 should enhance the efficacy of cytotoxic anti-cancer therapies. Indeed, the combination of AdVASH1 with CDDP did improve its efficacy.

In summary, VASH1 is selectively expressed in the ECs of tumor blood vessels. The expression is related to expression of angiogenic factors such as VEGF and FGF-2, and thus VASH1 can be further evaluated as an angiogenesis biomarker. Expression of endogenous VASH1 may participate in the inhibition of tumor angiogenesis, although it is not enough to block sprouting. However, exogenous VASH1 effectively inhibits sprouting angiogenesis, matures tumor vessels, and enhances antitumor efficacy when combined with conventional chemotherapy. We propose that VASH1 should be further tested in cancer diagnosis and therapy.

Acknowledgments

We thank Yuriko Fujinoya and Kyoko Shimizu for their excellent technical assistance.

References

1. Yano S, Matsumori Y, Ikuta K, Ogino H, Doljinsuren T, Sone S: Current status and perspective of angiogenesis and antivascular therapeutic strategy: non-small cell lung cancer. Int J Clin Oncol 2006, 11:73–81
2. Jain RK: Lessons from multidisciplinary translational trials on anti-angiogenic therapy of cancer. Nat Rev Cancer 2008, 8:309–316
3. Stinchcombe TE, Socinski MA: Bevacizumab in the treatment of non-small-cell lung cancer. Oncogene 2007, 26:3691–3698
4. Ferrara N, Kerbel RS: Angiogenesis as a therapeutic target. Nature 2005, 438:967–974
5. Bremnes RM, Camps C, Sirera R: Angiogenesis in non-small cell lung cancer: the prognostic impact of neoangiogenesis and the cytokines VEGF and bFGF in tumours and blood. Lung Cancer 2006, 51:143–158
6. Mattern J, Koomagi R, Volm M: Association of vascular endothelial growth factor expression with intratumoral microvessel density and tumour cell proliferation in human epidermoid lung carcinoma. Br J Cancer 1996, 73:931–934
7. Takanami I, Imamura T, Hashizume T, Kikuchi K, Yamamoto Y, Yamamoto T, Kodaira S: Immunohistochemical detection of basic fibroblast growth factor as a prognostic indicator in pulmonary adenocarcinoma. Jpn J Clin Oncol 1996, 26:293–297
8. Carmeliet P: VEGF as a key mediator of angiogenesis in cancer. Oncology 69 Suppl 2005, 3:4–10
9. Liao D, Johnson RS: Hypoxia: a key regulator of angiogenesis in cancer. Cancer Metastasis Rev 2007, 26:281–290
10. Swinson DE, O'Byrne KJ: Interactions between hypoxia and epidermal growth factor receptor in non-small-cell lung cancer. Clin Lung Cancer 2006, 7:250–256
11. Kandel J, Bossy-Wetzel E, Radvanyi F, Klagsbrun M, Folkman J, Hanahan D: Neovascularization is associated with a switch to the export of bFGF in the multistep development of fibrosarcoma. Cell 1991, 66:1095–1104
12. Sato Y: Update on endogenous inhibitors of angiogenesis. Endothelium 2006, 13:147–155
13. Dameron KM, Volpert OV, Tainsky MA, Bouck N: Control of angiogenesis in fibroblasts by p53 regulation of thrombospondin-1. Science 1994, 265:1582–1584
14. Fontanini G, Boldrini L, Calcinai A, Chine S, Lucchi M, Mussi A, Angeletti CA, Basolo F, Bevilacqua G: Thrombospondins I and II messenger RNA expression in lung carcinoma: relationship with p53 alterations, angiogenic growth factors, and vascular density. Clin Cancer Res 1999, 5:155–161
15. Yamaguchi M, Sugio K, Ondo K, Yano T, Sugimachi K: Reduced expression of thrombospondin-1 correlates with a poor prognosis in

patients with non-small cell lung cancer. Lung Cancer 2002; 36:143–150
16. Mascaux C, Martin B, Paesmans M, Verdebout JM, Verhest A, Vermylen P, Bosschaerts T, Ninane V, Sculier JP: Expression of thrombospondin in non-small cell lung cancer. Anticancer Res 2002; 22:1273–1277
17. Dudek AZ, Mahaseth H: Circulating angiogenic cytokines in patients with advanced non-small cell lung cancer: correlation with treatment response and survival. Cancer Invest 2005; 23:193–200
18. Watanabe K, Hasegawa Y, Yamashita H, Shimizu K, Ding Y, Abe M, Ohta H, Imagawa K, Hojo K, Maki H, Sonoda H, Sato Y: Vasohibin as an endothelium-derived negative feedback regulator of angiogenesis. J Clin Invest 2004; 114:898–907
19. Shibuya T, Watanabe K, Yamashita H, Shimizu K, Miyashita H, Abe M, Moriya T, Ohta H, Sonoda H, Shimosegawa T, Tabayashi K, Sato Y: Isolation and characterization of vasohibin-2 as a homologue of VEGF-inducible endothelium-derived angiogenesis inhibitor vasohibin. Arterioscler Thromb Vasc Biol 2006; 26:1051–1057
20. Shimizu K, Watanabe K, Yamashita H, Abe M, Yoshimatsu H, Ohta H, Sonoda H, Sato Y: Gene regulation of a novel angiogenesis inhibitor, vasohibin, in endothelial cells. Biochem Biophys Res Commun 2005; 327:700–706
21. Koizumi T, Abe M, Yamakuni T, Ohizumi Y, Hitotsuyanagi Y, Takeya K, Sato Y: Metronomic scheduling of a cyclic hexapeptide Ra-VII for anti-angiogenesis, tumor vessel maturation and anti-tumor activity. Cancer Sci 2006; 97:665–674
22. Kimura H, Miyashita H, Suzuki Y, Kobayashi M, Watanabe K, Sonoda H, Ohta H, Fujiwara T, Shimosegawa T, Sato Y: Distinctive localization and opposed roles of vasohibin-1 and vasohibin-2 in the regulation of angiogenesis. Blood 2009; 113:4810-4818
23. Yamashita H, Abe M, Watanabe K, Shimizu K, Moriya T, Sato A, Satomi S, Ohta H, Sonoda H, Sato Y: Vasohibin prevents arterial neointimal formation through angiogenesis inhibition. Biochem Biophys Res Commun 2006; 345:919–925
24. Li G, Tian L, Hou JM, Ding ZY, He QM, Feng P, Wen YJ, Xiao F, Yao B, Zhang R, Peng F, Jiang Y, Luo F, Zhao X, Zhang L, Zhou Q, Wei YQ: Improved therapeutic effectiveness by combining recombinant CXC chemokine ligand 10 with Cisplatin in solid tumors. Clin Cancer Res 2005; 11:4217–4224
25. Bardella C, Dettori D, Olivero M, Coltella N, Mazzone M, Di Renzo MF: The therapeutic potential of hepatocyte growth factor to sensitize ovarian cancer cells to cisplatin and paclitaxel in vivo. Clin Cancer Res 2007; 13:2191–2198
26. Kim SJ, Rabbani ZN, Dewhirst MW, Vujaskovic Z, Vollmer RT, Schreiber EG, Oosterwijk E, Kelley MJ: Expression of HIF-1α, CA IX, VEGF, and MMP-9 in surgically resected non-small cell lung cancer. Lung Cancer 2005; 49:325–335
27. McDonald DM, Foss AJ: Endothelial cells of tumor vessels: abnormal but not absent. Cancer Metastasis Rev 2000; 19:109–120
28. Bodey B, Bodey B Jr, Siegel SE, Kaiser HE: Immunocytochemical detection of endoglin is indicative of angiogenesis in malignant melanoma. Anticancer Res 1998; 18:2701–2710
29. Petrovic N, Bhagwat SV, Ratzan WJ, Ostrowski MC, Shapiro LH: CD13/APN transcription is induced by RAS/MAPK-mediated phosphorylation of Ets-2 in activated endothelial cells. J Biol Chem 2003; 278:49358–49368
30. St Croix B, Rago C, Velculescu V, Traverso G, Romans KE, Montgomery E, Lal A, Riggins GJ, Lengauer C, Vogelstein B, Kinzler KW: Genes expressed in human tumor endothelium. Science 2000; 289:1197–1202
31. van Beijnum JR, Dings RP, van der Linden E, Zwaans BM, Ramaekers FC, Mayo KH, Griffioen AW: Gene expression of tumor angiogenesis dissected: specific targeting of colon cancer angiogenic vasculature. Blood 2006; 108:2339–2348
32. Seaman S, Stevens J, Yang MY, Logsdon D, Graff-Cherry C, St Croix B: Genes that distinguish physiological and pathological angiogenesis. Cancer Cell 2007; 11:539–554
33. Yoshinaga K, Ito K, Moriya T, Nagase S, Takano T, Niikura H, Yaegashi N, Sato Y: Expression of vasohibin as a novel endothelium-derived angiogenesis inhibitor in endometrial cancer. Cancer Sci 2008; 99:914–919
34. Hanahan D, Folkman J: Patterns and emerging mechanisms of the angiogenic switch during tumorigenesis. Cell 1996; 86:353–364
35. Jain RK: Normalization of tumor vasculature: an emerging concept in antiangiogenic therapy. Science 2005; 307:58–62

blood

2009 113: 4810-4818
Prepublished online Feb 9, 2009;
doi:10.1182/blood-2008-07-170316

Distinctive localization and opposed roles of vasohibin-1 and vasohibin-2 in the regulation of angiogenesis

Hiroshi Kimura, Hiroki Miyashita, Yasuhiro Suzuki, Miho Kobayashi, Kazuhide Watanabe, Hikaru Sonoda, Hideki Ohta, Takashi Fujiwara, Tooru Shimosegawa and Yasufumi Sato

Blood (print ISSN 0006-4971, online ISSN 1528-0020), is published semimonthly by the American Society of Hematology, 1900 M St, NW, Suite 200, Washington DC 20036.

Distinctive localization and opposed roles of vasohibin-1 and vasohibin-2 in the regulation of angiogenesis

Hiroshi Kimura,[1,2] Hiroki Miyashita,[1] Yasuhiro Suzuki,[1] Miho Kobayashi,[1] Kazuhide Watanabe,[1] Hikaru Sonoda,[3] Hideki Ohta,[3] Takashi Fujiwara,[4] Tooru Shimosegawa,[2] and Yasufumi Sato[1]

[1]Department of Vascular Biology, Institute of Development, Aging, and Cancer, Tohoku University, Sendai; [2]Department of Gastroenterology, Tohoku University Graduate School of Medicine, Sendai; [3]Discovery Research Laboratories, Shionogi and Co, Osaka; and [4]Department of Biological Resources, Integrated Center for Science (INCS), Ehime University, Shitsukawa, Ehime, Japan

We recently isolated a novel angiogenesis inhibitor, vasohibin-1, and its homologue, vasohibin-2. In this study we characterize the role of these 2 molecules in the regulation of angiogenesis. In a mouse model of subcutaneous angiogenesis, the expression of endogenous vasohibin-1 was low in proliferating ECs at the sprouting front but high in nonproliferating endothelial cells (ECs) in the termination zone. In contrast, endogenous vasohibin-2 was preferentially expressed in mononuclear cells mobilized from bone marrow that infiltrated the sprouting front. When applied exogenously, vasohibin-1 inhibited angiogenesis at the sprouting front where endogenous vasohibin-1 was scarce but did not influence vascularity in the termination zone where endogenous vasohibin-1 was enriched. Exogenous vasohibin-2 prevented the termination of angiogenesis in the termination zone and increased vascularity in this region. Angiogenesis was persistent in the termination zone in the *vasohibin-1* knockout mice, whereas angiogenesis was deficient at the sprouting front in the *vasohibin-2* knockout mice. Supplementation of deficient proteins normalized the abnormal patterns of angiogenesis in the vasohibin knockout mice. These results indicate that vasohibin-1 is expressed in ECs in the termination zone to halt angiogenesis, whereas vasohibin-2 is expressed in infiltrating mononuclear cells in the sprouting front to promote angiogenesis. (Blood. 2009; 113:4810-4818)

Introduction

Angiogenesis, or the formation of new capillaries, is a key event in various developmental or remodeling processes that take place under physiologic and pathologic conditions. Angiogenesis is a dynamic phenomenon that involves sequential processes. The initial event is the detachment of mural pericytes from preexisting vessels for vascular destabilization. Subsequently, specialized endothelial cells (ECs) at the tip of sprout, called tip cells, degrade the basement membrane and extracellular matrices and actively migrate. The stalk cells follow the tip cells, proliferate, and form tubes. Finally, pericytes reattach to the new vessels as they mature. Through these processes, a new hierarchical vascular architecture will be constructed.[1]

The local balance between angiogenesis stimulators and inhibitors determines whether angiogenesis will be switched on. Numerous endogenous angiogenesis inhibitors are found in the body and play distinctive roles.[2] For example, molecules such as pigment epithelium-derived factor,[3,4] chondromodulin-1,[5,6] and maspin[7,8] are localized extrinsic to the vasculature and block the intrusion of new vessels as functional barriers. Thrombospondin-1 and thrombospondin-2 are deployed mainly by platelets and turn the angiogenic switch off.[9] Moreover, several angiogenesis inhibitors, including endostatin and tumstatin, are generated by the degradation of the basement membrane during angiogenesis.[10] Besides them, ECs themselves have the capacity to synthesize certain inhibitors that autoregulate angiogenesis.[2]

By searching for novel and functional vascular endothelial growth factor (VEGF)–inducible molecules in ECs, we isolated one angiogenesis inhibitor and named it vasohibin-1 (VASH1).[11] VASH1 is induced in cultured ECs by representative angiogenic growth factors, such as VEGF and fibroblast growth factor 2 (FGF-2), and is detected selectively in ECs at the site of angiogenesis in vivo.[11] The inducible expression of VASH1 in ECs is impaired by tumor necrosis factor-α, interleukin-1, or hypoxia.[11,12] Human VASH1 protein is composed of 365 amino acid residues. VASH1 lacks a classical secretion signal sequence but is released extracellulary, indicating that VASH1 is an unconventional secretory protein.[11,13] When applied exogenously, VASH1 inhibits the migration and proliferation of ECs stimulated with either VEGF or FGF-2.[11] This inhibitory effect is not due to the inactivation of growth factor signals, because VASH1 does not affect VEGF receptor 2 or ERK1/2 phosphorylation in ECs on VEGF simulation.[11] VASH1 exerts antiangiogenic activity under various pathologic conditions such as those of tumors, retinal neovascularization, and arterial intimal thickening, implying a possible clinical application.[11,14,15]

Through a DNA sequence search of genomic databases, we found one gene homologous to VASH1 and named it vasohibin-2 (VASH2).[16] The genes for human *VASH1* and *VASH2* are located on chromosome 14q24.3 and 1q32.3, respectively.[17] Human vasohibin-2 is composed of 355 amino acid residues, and the overall homology between human VASH1 and VASH2 is 52.5% at

Submitted July 23, 2008; accepted January 27, 2009. Prepublished online as *Blood* First Edition paper, February 9, 2009; DOI 10.1182/blood-2008-07-170316.

The online version of this article contains a data supplement.

The publication costs of this article were defrayed in part by page charge payment. Therefore, and solely to indicate this fact, this article is hereby marked "advertisement" in accordance with 18 USC section 1734.

the amino acid level. Similar to VASH1, any known functional motifs are found in the primary structure of VASH2.

The expression of VASH2 in cultured ECs is very low and is not inducible, but VASH1 and VASH2 proteins are comparably detected in ECs in the developing organs of embryos.[16] We have shown that VASH1 and VASH2 are diffusely expressed in ECs in embryonic organs during mid-gestation. After that time point, they become faint but persisted to a certain extent from late-gestation to neonate. Nevertheless, the function of these 2 molecules remained to be elucidated.

Here, we examined the roles of VASH1 and VASH2 in the regulation of postnatal angiogenesis in detail. For this purpose, we used a simple and reproducible model of postnatal angiogenesis in mice. To our surprise, the spatiotemporal expression patterns of VASH1 and VASH2 were distinct, with VASH1 present in ECs where angiogenesis terminated and with VASH2 present in bone marrow–derived mononuclear cells (MNCs) at the sprouting front. Furthermore, a loss-of-function experiment using knockout mice, as well as a gain-of-function experiment using adenovirus-mediated gene transfer, showed that VASH1 and VASH2 play distinctive roles in the regulation of angiogenesis.

Methods

Mouse model of hypoxia-mediated subcutaneous angiogenesis

All animal studies were reviewed and approved by the committee for animal study in the Institute of Development, Aging, and Cancer at Tohoku University.

A mouse model of subcutaneous angiogenesis was performed in accordance with the method described by Tepper et al.[18] Briefly, after anesthetization, bilateral incisions (2.5 cm in length and 1.25 cm in distance) were made on the dorsal skin of male C57BL/6 mice (Clea, Tokyo, Japan) that penetrated the cutis, dermis, and underlying adipose tissue. A silicon sheet was inserted beneath the flap, and the incisions were closed. In some experiments, adenovirus vector encoding the human *VASH1* gene (AdVASH1),[11] AdVASH2, or adenoviral vector encoding *β-galactosidase* gene (AdLacZ; 10^9 plaque-forming units was injected into the tail vein.[15] AdVASH2 was prepared in accordance with the method described.[11] Seven days after skin surgery, the mice were killed, and the skin flaps were collected for histologic analyses.

For the detection of hypoxic areas, mice were intravenously injected with pimonidazole (Chemicon International, Temecula, CA) 30 minutes before collecting the flap. Hypoxic areas were detected with the Hypoxyprobe-1 mAb1 (Chemicon International).

Generation of *VASH1* and *VASH2* knockout mice

For the construction of the *VASH1* targeting vector, a 7.6-kb genomic fragment upstream of exon 1 and a 2.4-kb genomic fragment downstream of exon 2 were subcloned. The region was designed such that the short homology arm (SA) extends 2.4 kb to 5′ end of loxP/FRT flanked Neo cassette, and the long homology arm (LA) starts at the 3′ side of loxP/FRT flanked Neo cassette. For the construction of the *VASH2* targeting vector, a 7.8-kb genomic fragment upstream of exon 3 and a 2.4-kb genomic fragment downstream of exon 3 were subcloned. The region was designed such that the SA extended 2.4 kb to the 5′ side of the Neo cassette, and the LA started at the 5′ side of LacZ cassette. The loxP/FRT flanked Neo cassette replaced 6.6 kb of the *VASH1* gene, including exon 1 (including the ATG start codon), whereas exon 3 of the *VASH2* gene was replaced with the LacZ/Neo cassette.

Targeted alleles were generated by homologous recombination in embryonic stem (ES) cells of C57BL/6 background. The ES cells carrying each of the targeted alleles were injected into C57BL/6 mouse blastocysts to produce chimeric mice. Chimeras were mated with C57BL/6 females to obtain F1 mice carrying each of the targeted alleles.

Immunohistologic analysis

For immunohistochemical analysis of the skin flap, specimens were frozen in OCT compound (Sakura, Tokyo, Japan), sliced into 10-μm sections, and fixed in methanol for 20 minutes at −20°C. Primary antibody reactions were performed at a dilution of 1:200 for CD31 (rat anti–mouse CD31 mAb; Research Diagnosis, Flanders, NJ), α smooth muscle actin (αSMA) (mouse anti–mouse αSMA mAb; Sigma-Aldrich, St Louis, MO), lymphatic vessel endothelial hyaluronate receptor 1 (LYVE-1; rabbit anti–mouse LYVE-1 polyclonal Ab; Acris Antibodies, Himmelreich, Germany), PCNA (mouse anti–mouse PCNA mAb; Santa Cruz Biotechnology, Santa Cruz, CA), CD11b (goat anti–mouse CD11b polyclonal Ab; Santa Cruz Biotechnology), and macrophage-specific antigen F4/80 (rat anti–mouse F4/80 mAb; Acris Antibodies) and at 1:400 for mouse VASH1 (rabbit anti–mouse VASH1 polyclonal Ab)[16] and VASH2 (rabbit anti–mouse VASH 2 polyclonal Ab)[16] overnight at 4°C. Specificities of anti–mouse VASH1 and anti–mouse VASH2 antibodies have been shown previously.[16] Secondary antibody reactions were performed at a dilution of 1:1500 of the appropriate Alexa 488–, Alexa 568–, or Alexa 594–conjugated donkey secondary Abs (Molecular Probes, Eugene, OR) for 1 hour at room temperature. The vascular luminal area was calculated from 5 different high-power fields.

For whole-mount immunohistochemical analysis of ear skin, the ear skin was prepared according to the method described by Oike et al.[19] Briefly, ear skin was fixed with 4% paraformaldehyde in PBS for 2 hours, permeabilized with methanol, and blocked in 5% sheep serum in 0.3% Triton X-100 (Sigma-Aldrich) in PBS. Primary antibodies and secondary antibodies were incubated overnight at 4°C.

All the samples were analyzed with a Fluoview FV1000 confocal fluorescence microscope (Olympus, Tokyo, Japan) with an UPLSAP 10× or 40× objective lens at room temperature. Fluorochromes used were Alexa 488, Alexa 594, fluorescein isothiocyanate (FITC), or green fluorescent protein (GFP). We used Olympus Fluoview software.

Scanning electron microscopy

Ear skin was obtained and fixed with 3% glutaraldehyde in 0.1 M phosphate buffer (pH 7.4). The method of scanning electron microscopy (SEM) observation was as previously reported.[20] In brief, the specimens were treated with 1% to 2% sodium hypochlorite solution for 45 to 100 seconds, hydrolyzed with 8N HCl for 30 minutes, postfixed with 1% OsO_4, treated with 1% tannic acid solution, and again with 1% OsO_4. After a brief rinse, the specimens were dehydrated through a graded series of ethanol, immersed in t-butyl alcohol, freeze-dried, coated with platinum, and observed with an SEM (Hitachi S-800; Hitachi, Tokyo, Japan).

Detection of vessel perfusion

For the detection of blood vessels with perfusion, mice were infused with FITC-labeled concanavalin A (Sigma-Aldrich) by intracardiac injection before the collection of skin flap. Thereafter, samples were analyzed using a confocal fluorescence microscope (Olympus).

Bone marrow transplantation

Wild-type mice were lethally irradiated with 1 dose of 9 Gy. Thereafter, bone marrow cells harvested from GFP-mice (generous gift from Dr Okabe, Osaka University, Osaka, Japan) that had been purified by density centrifugation (Ficoll-paque PLUS; Amersham Biosciences, Uppsala, Sweden), were transplanted into the wild-type mice (5×10^6 cells/animal). All the recipient mice were given a minimum of 6 weeks of rest to allow for complete bone marrow reconstitution. The engraftment efficiency was determined by fluorescence-activated cell sorting (FACS; FACS Vantage; Becton Dickinson, San Jose, CA) for GFP expression in the bone marrow of mice receiving transplants of GFP-positive bone marrow cells.

Cells

Human umbilical vein endothelial cells (HUVECs) were obtained from KURABO Industries (Osaka, Japan) and were cultured on type-I collagen–coated dishes (IWAKI, Chiba, Japan) in 10% fetal bovine serum (FBS)/

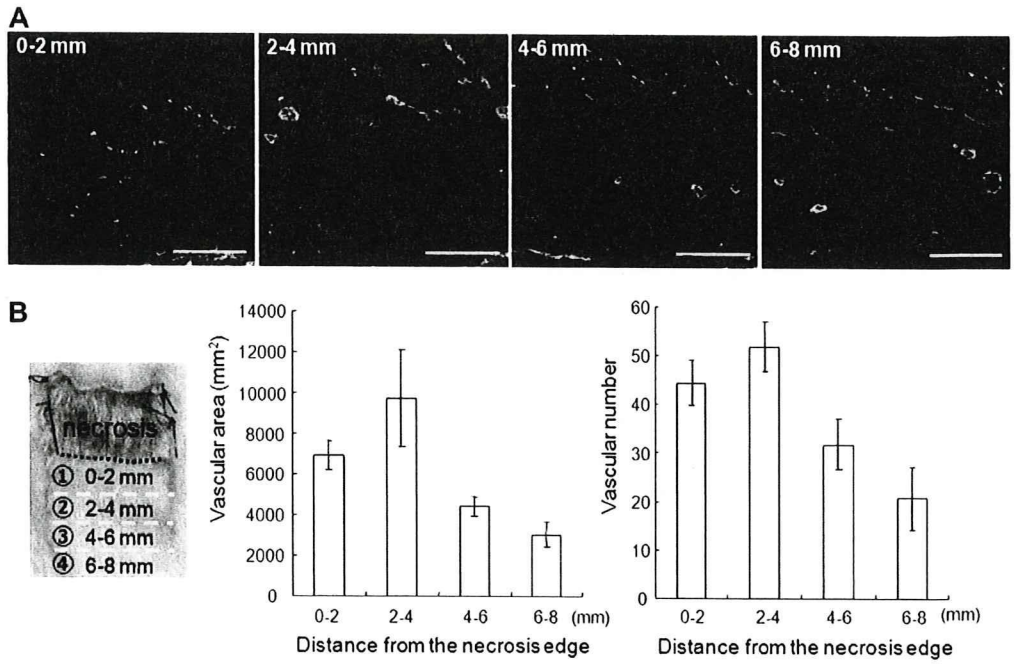

Figure 1. New vessel distribution in the skin flap. (A) The vascular distribution in the skin flap was observed in areas at every 2-mm interval from the necrotic edge. CD31 (red) is a marker for ECs, and αSMA (green) is a marker for mural cells. Scale bars are 200 μm. (B) The dashed line indicates the necrotic edge. The vascular area and vascular density per high-power field were determined from every 2-mm interval from the necrotic edge. Data are expressed as the means and SDs of each area.

endothelial basal medium (Clonetics, Walkersville, MD). THP-1, a human monocytic cell leukemia cell line was obtained from the Cell Resource Center for Biomedical Research at our institute. THP-1 cells were cultured in 10% FBS/RPMI 1640 (Nissui Pharmaceutical, Tokyo, Japan). GM7373, a chemically immortalized bovine aortic endothelial cell line, was cultured in Dulbecco modified Eagle medium (Nissui Pharmaceutical) supplemented with 10% FCS. MS1, an immortalized cell line with a SV40 large T antigen from mouse pancreatic ECs, was purchased from ATCC (Manassas, VA) and were cultured in αMEM (Invitrogen, Carlsbad, CA) supplemented with 10% FCS. All the cells were cultured at 37°C in a humidified atmosphere with 5% CO_2.

Reverse transcriptase-polymerase chain reaction analysis

Total RNA was extracted from HUVECs and THP-1 cells by the AGPC method using ISOGEN (Nippon Gene, Toyama, Japan) according to the manufacturer's instructions. Total tissue RNA was extracted from several organs of male BALB/c mice at 4 weeks or from placentas of female BALB/c mice by the AGPC method using ISOGEN-LS (Nippon Gene). First-strand cDNA was generated using a first-strand cDNA synthesis kit for reverse transcriptase–polymerase chain reaction (RT-PCR; Roche Diagnostics, Mannheim, Germany). RT-PCR was performed with a DNA thermal cycler (Takara, Tokyo, Japan). PCR conditions consisted of an initial denaturation step at 95°C for 10 minutes followed by 40 cycles consisting of 15 seconds at 95°C, 5 seconds at an indicated annealing temperature, and 15 seconds at 72°C. The primer pairs used were as follows: mouse β-actin forward, 5-ACAATGAGCTGCGTGTGGCT, and reverse, 5-TCTCCTTA-ATGTCACGCACGA (annealing temperature 58°C); mouse VASH1 forward, 5-AGATCCCCATACCGAGTGTG, and reverse, 5-GGGCCTCTTT-GGTCATTTCC (annealing temperature 58°C); mouse VASH2 forward, 5′-ATGCCTTGAAGCTGTCATCC, and reverse, 5′-TGGCATATTTCTC-CAGCTCC (annealing temperature 60°C). PCR products were analyzed by 1% or 1.5% agarose gel electrophoresis.

Quantitative real-time RT-RCR

Total RNA was extracted from the skin flap using the RNeasy Mini Kit (QIAGEN, Valencia, CA) according to the manufacturer's instructions. First-strand cDNA was generated with a first-strand cDNA synthesis kit for RT-PCR (Roche Diagnostics). Quantitative real-time RT-PCR was performed with the use of a Light Cycler System (Roche Diagnostics) according to the manufacturer's instructions. The amount of PCR product was measured as a fluorescence signal that was proportional to the amount of the specific target sequence present. PCR conditions consisted of an initial denaturation step at 95°C for 10 minutes, followed by 40 cycles consisting of 15 seconds at 95°C, 5 seconds at an indicated annealing temperature, and 15 seconds at 72°C. The primer pairs used were as follows: β-actin forward, 5-TCGTGCGTGACATCAAAGAG, and reverse, 5-TGGACAGT-GAGGCCAGGATG; mouse VASH1 forward, 5-GATTCCCATACCAAGTGT-GCC, and reverse, 5-ATGTGGCGGAAGTAGTTCCC (annealing temperature 62°C); mouse VASH2 forward, 5′-GGCTAAGCCTTCAATTCCCC, and reverse, 5′ CCCATTGGTGAGATAGATGCC (annealing temperature 64°C). Each mRNA level was measured as a fluorescent signal corrected according to the signal for β-actin.

Northern blot analysis

Northern blotting was performed as described.[11] Briefly, cells were starved in 0.1% FBS/αMEM. In some experiments, cells were stimulated with VEGF (Sigma-Aldrich) for 12 hours. Total RNA was then extracted by ISOGEN according to the manufacturer's instruction and was separated on a 1% agarose gel containing 2.2 M formaldehyde and transferred to a Hybond N^+ membrane. The membrane was hybridized with a ^{32}P-labeled VASH1 cDNA probe containing an open reading frame (464-1417). Autoradiography was performed on an imaging plate and analyzed with an FLA2000 (Fuji Film, Tokyo, Japan).

Intracellular localization of VASH1 and VASH2

To make a hemagglutinin (HA)–tagged construct, human VASH2 cDNA was cloned into the *Eco*R1-*Xho*1 site of internal ribosome entry site (IRES)–humanized Renilla green fluorescent protein (hrGFP) 2a vector (Stratagene, La Jolla, CA; VASH2, HA-IRES-GFP vector). To make GFP-fusion constructs, human VASH2 cDNA was cloned into CT-GFP TOPO vector (VASH2, CT-GFP vector) or NT-GFP TOPO vector (VASH2, NT-GFP vector; Invitrogen). Transfection was performed with Fugene 6 (Roche) according to the manufacturer's instructions. GFP-fusion protein was detected by the use of confocal microscopy.

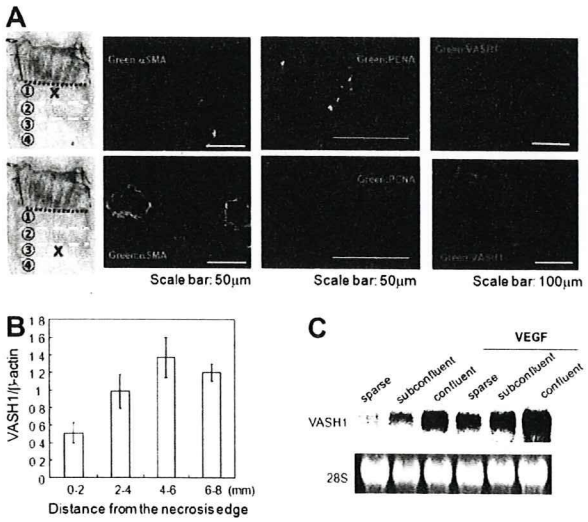

Figure 2. The spatiotemporal expression profile of VASH1. (A) Immunostaining of CD31 (red), αSMA (green), PCNA (green), and/or VASH1 (green) was performed with the indicated area of the skin flap. (B) Total RNA was isolated from each area of the skin flap. Quantitative real-time RT-PCR was performed to show mRNA levels of VASH1 in each area. Each value was standardized with β-actin. Data are expressed as mean and SDs. (C) HUVECs of sparse, subconfluent, and confluent conditions were treated with or without VEGF (1 nM) for 12 hours, and the expression of VASH1 was determined by Northern blotting.

Establishment of VASH1- or VASH2-expressing MS1 clones

To improve the activity of transcription, the CMV promoter of the pcDNA3.1/Hygro plasmid (Invitrogen) was replaced with the chicken β-actin promoter derived from pCALL2.[21] This vector, pCALL2-pcDNA3.1/Hygro, was used for the transfection in this study. Human VASH1 or VASH2 cDNA was cloned into the pCALL2-pcDNA3.1/Hygro vector at multiple cloning sites (*Xho*-I and *Not*-I). MS1 was transfected with the expression vector with the use of the Effectene transfection reagent (QIAGEN) according to the manufacturer's protocol. After the transfection, the cells were selected by hygromycin (500 μg/mL; Invitrogen).

Statistical analysis

The statistical significance of differences was evaluated by unpaired analysis of variances, and probability values were calculated with the Student *t* test. A value of P less than .05 was considered statistically significant.

Results

Mouse model of postnatal subcutaneous angiogenesis

To explore the roles of VASH family in the regulation of angiogenesis, we used a mouse model of postnatal subcutaneous angiogenesis. In this model, 2 parallel skin incisions were made on the back that penetrated the cutis, dermis, and underlying adipose tissue; a silicon sheet was inserted beneath the skin flap; and the incision was closed (Figure S1A, available on the *Blood* website; see the Supplemental Materials link at the top of the online article). The skin flap became hypoxic because the inserted silicon sheet blocked the blood supply from the deeper layer, and new vessels were distributed from the areas left undissected. Because of the substantial length of the skin incision, the central region became necrotic over the experimental period (Figure S1B). After 7 days, the skin flap was harvested and oriented parallel to the original incision for sectioning (Figure S2A). Pimonidazole staining showed that hypoxia was evident at the edge adjoining the necrotic tissue (Figure S2B).

We evaluated the skin flap at every 2-mm interval from the necrotic edge and determined the vessel distribution in each area (Figure 1A). In this way, the entire progress of angiogenesis could be observed from a single section. The area 0 to 4 mm from the necrotic edge contained mostly small vessels with PCNA-positive proliferating ECs (Figure 1A). This area was thus defined as the sprouting front of angiogenesis. The elevation of vascular luminal area and vascular numbers was most prevalent in the area 2 to 4 mm from the necrotic edge (Figure 1B). The area further than 4 mm from the necrotic edge contained hierarchical vasculature of small and large vessels with PCNA-negative nonproliferating ECs surrounded by αSMA-positive mural cells (Figure 1A). This area was thus defined as the termination zone of angiogenesis. Vascular luminal area and vascular numbers were decreased in this area (Figure 1B).

Spatiotemporal expression profile of VASH1 and VASH2 during angiogenesis

During the postnatal period, the expression of VASH1 and VASH2 proteins is only faintly shown in arterial ECs under the basal condition.[16] Here, we determined VASH2 mRNA in various organs

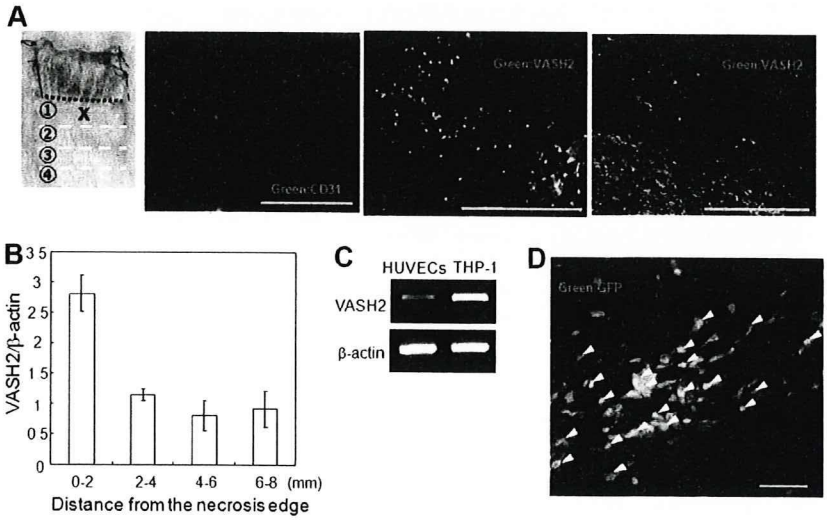

Figure 3. The spatiotemporal expression profile of VASH2. (A) Immunostaining of VASH2, CD11b, and F4/80 in the area 0 to 2 mm from the necrotic edge. Scale bars are 200 μm. (B) Total RNA was isolated from each area of the skin flap. Quantitative real-time RT-PCR was performed to show mRNA levels of VASH2 in each area. Each value was standardized with β-actin. (C) The basal level of VASH2 mRNA in HUVECs or THP-1 cells was determined by RT-PCR. (D) After confirming bone marrow reconstitution, the subcutaneous angiogenesis experiment was performed. Immunostaining of VASH2 in the area 0 to 2 mm from the necrotic edge is shown. Arrowheads indicate GFP-positive and VASH2-positive cells. Scale bar is 50 μm.

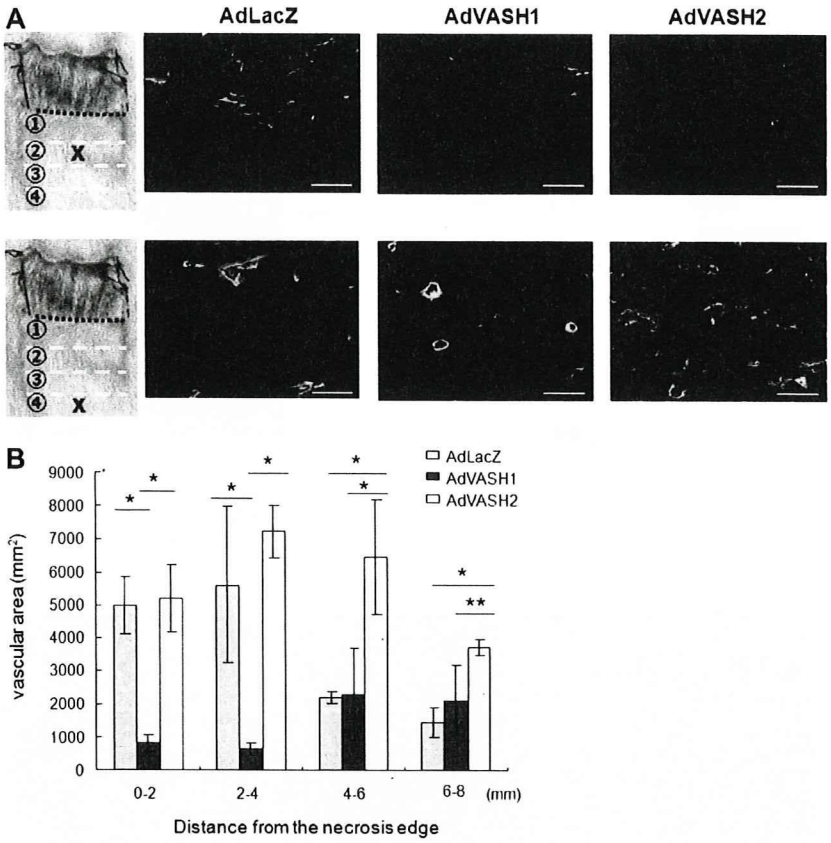

Figure 4. Effects of exogenous VASH1 or VASH2 on angiogenesis in the skin flap. AdVASH1 or AdVASH2 was injected into the tail vein to supply sufficient exogenous proteins to the site of angiogenesis. (A) Immunostaining of CD31 (red) and αSMA (green) positive cells in the indicated area of the skin flap. Scale bars are 50 μm. (B) Vascular area was determined from 5 different fields in each area. Data are expressed as the means and SDs; $^{*}P < .01$, $^{**}P < .05$.

in mice (Figure S3). This restricted expression pattern of VASH2 was comparable with that of VASH1,[11] and it further confirmed that basal expression of these 2 proteins is quite low. However, we have already reported that VASH1 is selectively present in ECs at the site of angiogenesis.[11,14,15]

Here, we determined their expression during angiogenesis more precisely. Immunostaining of VASH1 protein showed that PCNA-positive ECs in small vessels at the sprouting front were faintly stained, whereas PCNA-negative ECs surrounded by mural cells in the termination zone were intensely stained (Figure 2A). Quantitative real-time RT-PCR further confirmed that VASH1 mRNA was lowest in the area 0 to 2 mm from the necrotic edge, increased and was most prevalent in the area of 4 to 6 mm from the necrotic edge, and then declined thereafter (Figure 2B). Because VASH1 was identified as a VEFG-inducible molecule,[11] we initially thought that ECs in the sprouting front expressed VASH1 abundantly. However, it was not the case. We therefore reevaluated the expression pattern of VASH1 by using cultured HUVECs. What we found was that the expression level of VASH1 was dependent on the culture conditions. The basal expression of VASH1 in exponentially proliferating HUVECs was extremely low, increased in subconfluent to confluent cultures, although VEGF-inducibility was maintained (Figure 2C). Thus, the expression profile of VASH1 in the skin flap correlated with what we found in the culture condition.

We then determined the expression of VASH2 in this system. We noted that VASH2 protein was preferentially localized in infiltrating MNCs in the area 0 to 2 mm from the necrotic edge (Figure 3A). These MNCs were CD11b-positive but F4/80-negative (Figure 3A). Although we showed the specificity of our antibodies previously,[16] the specificity was further confirmed, because VASH1 was negative in MNCs in the sprouting front (Figure 2A), whereas VASH2 was negligible in ECs in the termination zone (Figure S4). Quantitative real-time RT-PCR further confirmed that VASH2 mRNA was highest in the area 0 to 2 mm from the necrotic edge (Figure 3B). We could also show that monocytic TPH-1 cells expressed VASH2 mRNA more abundantly than HUVECs (Figure 3C).

It has been well accepted that bone marrow–derived cells contribute to angiogenesis.[22] We therefore hypothesized that these MNCs were derived from bone marrow. To prove this, we lethally irradiated wild-type mice and transplanted them with bone marrow cells from mice ubiquitously expressing green fluorescent protein (GFP-mice). After confirming bone marrow reconstitution, we performed the subcutaneous angiogenesis analysis. We observed that most of the VASH2-positive MNCs were positive for GFP (Figure 3D arrowheads). We could hardly detect GFP-positive cells integrated in the wall of neo-vessels.

These results indicate that VASH1 is expressed by ECs in the termination zone, whereas VASH2 is mainly expressed by bone marrow–derived MNCs infiltrating the sprouting front.

Effects of exogenous VASH1 or VASH2 on angiogenesis

To evaluate the effect of exogenous VASH1 or VASH2, we injected AdVASH1 or AdVASH2 into the tail vein of mice to cause expression of these genes in the liver. We confirmed the expression of VASH1 or VASH2 in the liver (data not shown). As described previously, this procedure supplied sufficient proteins to regulate angiogenesis in the remote site.[15] Adenovirus-mediated transfer of the *VASH1* gene inhibited angiogenesis at the sprouting front where endogenous VASH1 was scarce, but it did not influence vascularity in the termination zone where endogenous VASH1 was enriched (Figure 4A,B). Adenoviral-mediated transfer of the *VASH2* gene

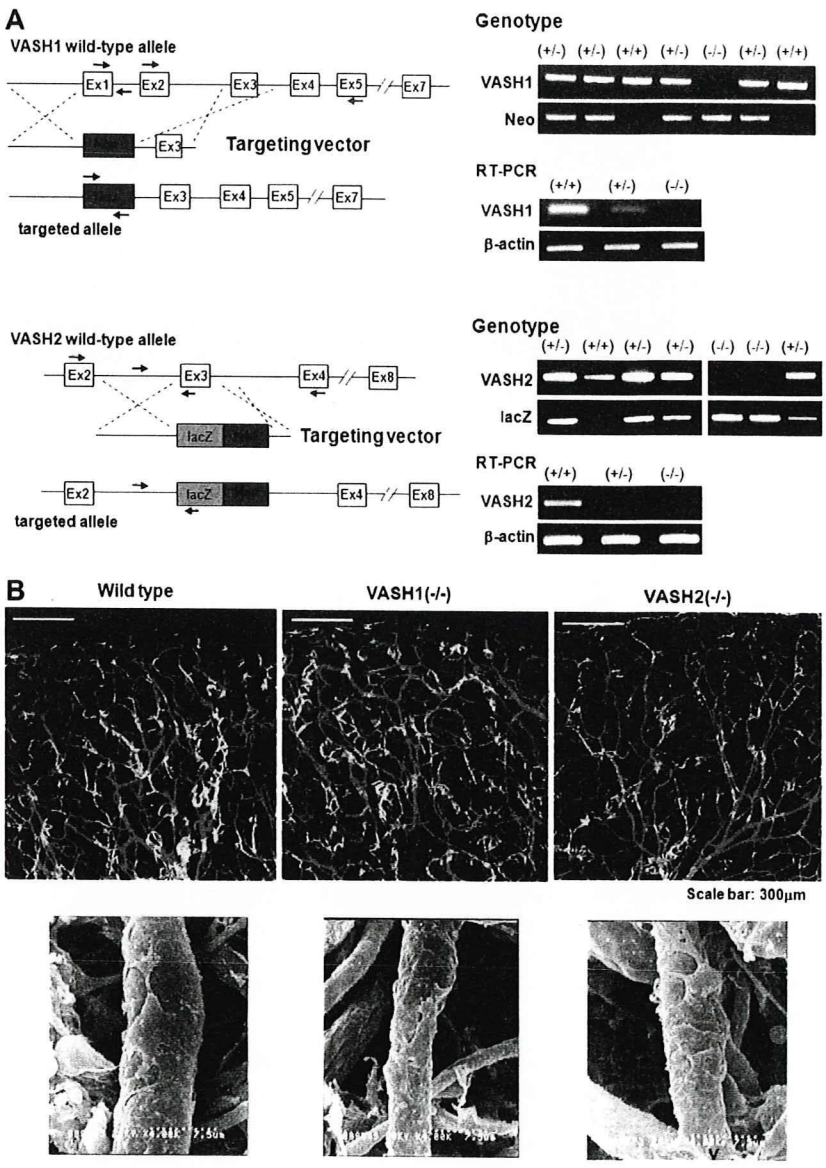

Figure 5. Generation of *VASH1* and *VASH2* knockout mice and their steady state subcutaneous vascular architecture. (A) *VASH1* and *VASH2* knockout mice were generated as described in "Generation of VASH1 and VASH2 knockout mice." Genotyping and the analysis of each transcript by RT-PCR are shown. (B) Ear skin was used to show the steady state vascular architecture of ear skin. Top panels show immunostaining of CD31 (green) and LYVE-1 (red). Bottom panels show SEM of capillary vessels.

did not cause any changes in the sprouting front, but it sustained the increased vascularity in the termination zone (Figure 4A,B). These opposing effects of VASH1 and VASH2 were further confirmed in vitro by the stable transfection of the *VASH1* or *VASH2* gene into cultured ECs (Figure S5). Both VASH1 and VASH2 lack classical signal sequences.[11,16] We have previously shown that VASH1 is an endoplasmic reticulum–independent secretory protein. To compare the intracellular localization of VAS1 and VASH2 proteins, we constructed the GFP-fused human *VASH2* expression vectors and transfected them into GM7373 cells. We simultaneously transfected human *VASH1* gene with the use of AdVASH1. As shown in Figure S6, the intracellular localization of VASH1 and VASH2 was comparable. In consequence, exogenous VASH1 inhibits angiogenesis at the sprouting front, whereas exogenous VASH2 prolongs angiogenesis in the termination zone.

Function of endogenous VASH1 or VASH2 on angiogenesis

To further clarify the function of endogenous VASH1 and VASH2, we generated *VASH1* or *VASH2* knockout mice by conventional homologous recombination (Figure 5A). We examined the steady state vascular architecture of ear subcutis of survived mice. We could not find any significant changes of vascular architecture in either *VASH1* knockout or *VASH2* knockout mice (Figure 5B).

We then subjected the *VASH1* knockout and *VASH2* knockout mice to the model of subcutaneous angiogenesis. The degree of vascular area at the sprouting front was almost identical between wild-type, $VASH1^{+/-}$, and $VASH1^{-/-}$ mice (Figure 6B). The vascular area significantly decreased in the termination zone in the wild-type mice where endogenous VASH1 was enriched, but that was maintained in higher degree in *VASH1* knockout mice (Figure 6A). Quantitative analysis showed that this change was gene-dosage sensitive (Figure 6B). Lectin staining indicated that new vessels of $VASH1^{-/-}$ mice were patent and maintained blood flow (Figure 6C). Supplementation of the deficient proteins by adenoviral-mediated gene transfer normalized the abnormal angiogenesis patterns in *VASH1* knockout (Figure 6D).

In contrast, the vascular density was lower in entire areas in the *VASH2* knockout mice (Figure 7B). This change was gene-dosage